Table 1 Classification of fibrin networks formed by dysfibrinogens

Network class	Clot turbidity (A_{350})	Fiber width (nm)	Fiber length	Number of fiber ends*	Fiber packing, space or pores in the network
Normal	0.33–0.35	75–120	Long (> 10 μm) fibers with few branched fibers	< 3	Uniform packing
Less-ordered	0.31–0.35	75–120	Long (> 10 μm) fibers with few branched fibers	< 10	Slightly disturbed packing with tangled regions and spaces
Porous A	0.28–0.32	60–120	Long (> 10 μm) and short (2–5 μm) branched fibers	50–100	Disturbed packing with large pores or spaces
Porous B	0.16–0.22	30–80	Short (0.5–10 μm) highly branched fibers	> 100	Disturbed uniform packing with many large and small pores
Lace-like	0.11–0.20	15–30	Short (< 0.6 μm) highly branched fibers	< 3	Uniform packing with no spaces or pores

*In the 165 μm^2 are of 4500-fold magnified fibrin images.

Table 2 Characteristics of the abnormal fibrins formed by dysfibrinogens

Mutation	Network class	Compaction (%)	Permeation constant (10^{-9} cm^2)	Location name
Fibrin composed of normal thickness fibers:				
Normal fibrin		2.0–4.8	2.5–5.8	
AαE11G	Normal	ND	ND	Mitaka
AαR16C	Normal-like	3.3	ND	Tochigi II, Tokyo III and VIII
AαR16C	Less-ordered	7.3*, 9.3**	6.3*, 5.2**	Asahikawa IV*, Tokyo IV**
		ND	ND	Kawaguchi, Tokyo VI-VII
AαR16H	Normal	3.1*	3.5*	Hamasaka, Oita*, Osaka IV
AαG17V	Normal	ND	ND	Bremen
AαP18L	Normal	ND	ND	Kyoto II
AαR19G	Normal	2.6	2.7	Kumamoto
βN160S(CHO)	Less-ordered	4.3	0.29–3.8	Niigata
γC139Y	Normal	ND	ND	Pretoria
γG268E	Less-ordered	ND	ND	Kurashiki
γR275C	Porous A	18.3*, 21.8**	12.2*, 11.5**	Asahikawa II* and III**
		ND	ND	Morioka I-II, Osaka II, Tenri Tochigi I, Tokyo II
γR275H	Porous A	10.8	ND	Osaka III, Saga
γR275S	Less-ordered	5.3	ND	Kamogawa
γD330Y	Less-ordered	4.1	ND	Kyoto III
γR375G	Porous A	4.5	ND	Osaka V
Fibrin composed of thin fibers:				
AαR141S(CHO)	Porous B	18.3	ND	Lima (homozygous)
AαP343N(CHO)	Porous B	ND	ND	Caracas II
αC truncation	Lace-like	1.5	Not permeated	Marburg (homozygous)
αC truncation	Lace-like	2.2	Not permeated	Giessen (homozygous)
βC extension	Lace-like, porous B	24.5	Damaged	Osaka VI
γM310T(CHO)	Porous B	24.8	Damaged	Asahi
γA327T(CHO)	Porous B	> 25	Damaged	Tokyo V

Compaction and permeation data marked with * were taken from the respective Fbn location name marked with **.
The permeation data for Fbn Niigata were taken from [18].
ND, not determined; (CHO): extra-glycosylated.

with each other and small spaces or pores inside the networks (Figs 2 and 3). The compaction and permeation activities of the networks in this category were within the normal ranges, except for two of the AαR16C fibrins, Fbn Asahikawa IV and Fbn Tokyo IV, which showed higher compaction (7.3% and 9.3%, respectively) and slightly higher permeation (6.3×10^{-9} cm^2 and 5.2×10^{-9} cm^2, respectively) than the normal networks (2.0–4.8% and $2.5–5.8 \times 10^{-9}$ cm, respectively). Upon detailed observation, we observed many thin fibers tangled with the normal thickness fibers at each of the nodes of the AαR16C fibrins (Fig. 2H–J). Furthermore, the numbers and extents of the thin fibers in the network varied among the AαR16C fibrins, and a slightly wider deviation of the fiber width was noted. Representative fibrin images that were classified as normal and less-ordered networks are shown in Figs 2 and 3. From these results, we concluded that the dysfibrinogens with a defect in fibrinopeptide A (FPA) release or a defect in E:D binding as a result of alteration in either the 'A-knob' or 'a-hole'

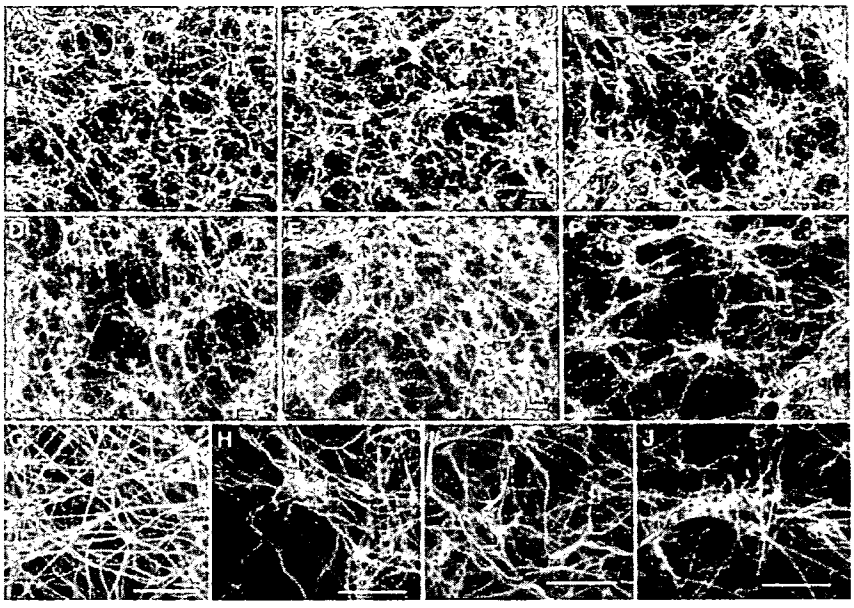

Fig. 2. Fibrin networks from AαR16 mutant fibrins. (A and G) normal fibrin; (B) AαR16H Fbn Hamasaka; (C and I) AαR16C Fbn Kawaguchi; (D and H) AαR16C Fbn Tokyo IV; (E) AαR16C Fbn Tochigi II; (F and J) AαR16C Asahikawa IV. Bars = 2 μm.

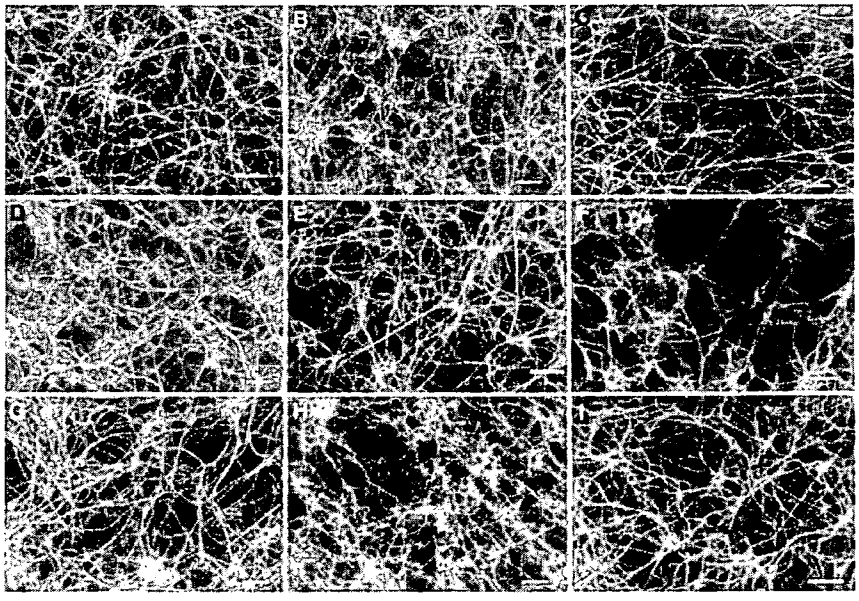

Fig. 3. Fibrin networks composed of normal thickness fibers. (A) normal fibrin; (B) AαG17V; (C) AαP18L; (D) AαR19G; (E) γG268E; (F) γR275C Asahikawa II; (G) γD330Y; (H) γR375G; (I) AαR141S(CHO). Bars = 2 μm.

region formed normal-like fibrin networks with similar characteristics to that of normal fibrin. The third category of fibrins, porous A fibrins, was distinct from the less-ordered fibrins on the basis of their fiber branching tendency, network architecture, compaction and permeability activity. The porous A fibrins were composed of a mixture of long (more than 10 μm) normal thickness fibers and short (2–5 μm) branched fibers, the latter of which often terminated in tapered or torn-off ends (Figs 3F,H and 4), as first demonstrated in the case of Fbn Tokyo II [15]. The dysfibrinogens that formed porous A fibrin networks were all γR275C, γR275H and γR375G fibrinogens. Although these fibrins had similar network architectures, their compactions varied and were found in the normal (4.1% for γR375G), high (10.8% for γR275H) and markedly high (18–21% for γR275C) ranges. These differences appeared to be caused by the extent of impairment of the D:D association, as

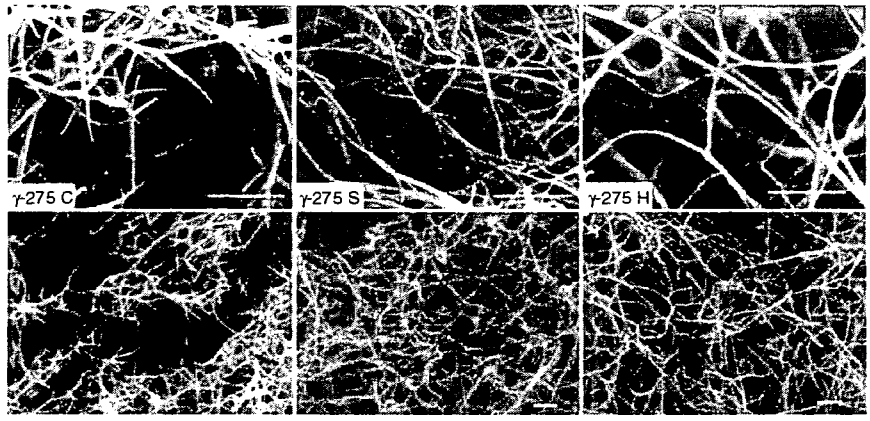

Fig. 4. Three types of γR275 mutant fibrins. All the γR275 mutant fibrins, namely γR275C (Asahikawa III), γR275S and γR275H (Saga), are composed of normal thickness fibers with tapered ends. The tapering tendency differs among the three types of mutations. The upper panels show close-up views at 9000-fold magnification. Bars = 2 μm.

γR275 is located at the D:D interface and plays a critical role in the D:D association, whereas γR375 is not located at or near the D:D interface but resides at the back of the E:D binding site and participates in the Ca^{2+} binding [28] that maintains the protein integrity. It should be noted that all the γR275C fibrins were indistinguishable from each other, but clearly different from the γR275H fibrins. Two of the γR275H fibrin networks contained tapered fibers but with far fewer fiber ends and spaces than the γR275C fibrins, and there were hardly any tapered fibers in the γR275S fibrin, which was classified as a less-ordered fibrin. When the four γ275 fibrins were compared, the incidences of the tapered fibers were in good agreement with their compaction ranges, namely very high compaction (18–21%) for the Cys mutant, high compaction (10.8%) for the His mutant (10.8%) and slightly high compaction (5.3%) for the Ser mutant, as compared with the normal Arg fibrin (< 4%, Table 2). After the compaction experiment, many of the γR275 mutant networks were completely compressed and broken, whereas the normal network of γR275 retained its structure, although it was slightly compressed. From these results, we concluded that a defect in the D:D association was more critical than a defect in the E:D association for the formation of the normal fibrin architecture.

Fibrin network structures composed of thin fibers

The turbidity of the clots was related to the fiber width, and clots with less than two-thirds the turbidity level of the normal clots, such as Fbn Marburg (αC-truncation, A_{350} = 0.11), Giessen (αC-truncation, A_{350} = 0.15), Osaka VI (βC-extension, A_{350} = 0.20), AαR141S (extra-glycosylated, CHO, A_{350} = 0.16), γM310T(CHO) (A_{350} = 0.20), AαP343N(CHO) (A_{350} = 0.21) and γA327T(CHO) (A_{350} = 0.22), were classified as category (B). The fibrin networks of these dysfibrinogens were composed of highly branched thin fibers, and further classified as lace-like or porous B on the basis of the network porosity. Lace-like networks were observed for the αC truncated or βC-elongated fibrins, while porous B networks were observed for the extra-glycosylated fibrins. In the lace-like networks, markedly thin fibers were highly branched and connected with each other to form three-dimensionally uniform networks with no pores or spaces inside (Fig. 5). Furthermore, the fiber widths were in a narrow range of 15–30 nm and no fibers of greater than 60 nm in width were present (Fig. 1B). However, the fiber length between the branch points varied from 100–200 nm in Fbn Marburg, 300–600 nm in Fbn Giessen and 400–600 nm in Fbn Osaka VI, although longer fibers of more than 600 nm without branches were not observed. It should be noted that both the αC truncated fibrins exhibited normal compaction, but no permeation of the fluid within the time of the experiments in each of two different experiments. We classified Fbn Osaka VI as a lace-like network, although we also observed a few regions of porous

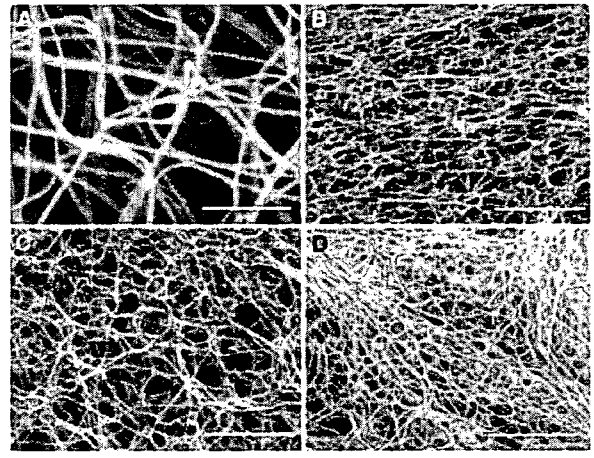

Fig. 5. Lace-like fibrin networks composed of highly branched thin fibers. (A) normal fibrin; (B) Fbn Marburg (αC truncation, bridged with albumin); (C) Fbn Giessen (αC truncation, bridged with albumin); (D) Fbn Osaka VI (βC extension). Bars = 1 μm.

B network within its network. We consider that Fbn Osaka VI primarily forms a lace-like network, but its structure becomes disturbed and forms porous regions at sites of mechanical stress, because of the weakness of the fibers [20]. In fact, the compaction of Fbn Osaka VI was positioned in the highest group (24.5%) and the network was easily damaged to form large pores when fluids were allowed to pass through the gel.

In the Porous B networks, the fiber width was in the range of 30–80 nm, and the branching tendency was lower than in the lace-like networks. The porous B networks were composed of mixed fiber lengths (500 nm to 10 μm), and contained many small and large pores with secondary networks composed of thinner fibers, such that the uniform fiber packing was disturbed (Fig. 6). Although we did not observe any regulation of the size and number of large pores in each porous B network, we could distinguish these networks by the extent of their branching tendency and the presence of fused thick fibers. However, the thin fibers appeared to be highly adhesive, and we often observed a few thicker fibers (80–100 nm), particularly at the boundary of the large pores, that seemed to be formed by adhesion and fusion of the thin fibers upon pore formation. The branching tendency in this group was higher than that of normal fibrin but lower than that of the lace-like networks, as long (< 1 μm) fibers without any branches were often observed (Fig. 6). Table 2 shows that as the number of large pores increased, the fibrin showed higher compaction [18.3% for AαR141S (CHO), 24.8% for γM310T(CHO) and > 25% for γA327T(CHO)], and the networks were easily damaged in the permeation or compaction experiments. From these results, we concluded that this type of fibrin was mostly fragile against mechanical stress, and that fragility of the network was associated with porous B networks but not lace-like networks.

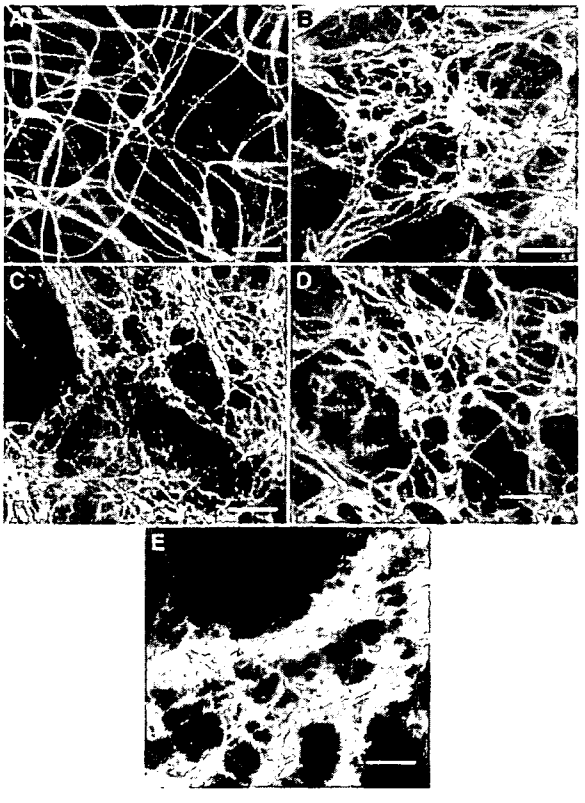

Fig. 6. Porous B fibrin networks composed of highly branched thin fibers. (A) normal fibrin; (B) γM310T(CHO); (C) AαR141S(CHO); (D) γA327T(CHO); (E) AαP343N(CHO). Bars = 1 μm.

Discussion

It is well known that the structure of fibrin clots is highly dependent on the fibrinogen and thrombin concentrations, ionic strength, pH, divalent metal ions, negatively charged substances and some plasma proteins, such as albumin, and that slight changes in these factors causes the formation of abnormal fibrin clots, even in reactions between normal fibrinogen and thrombin. Several dysfibrinogens have been reported to form abnormal fibrin clots, which are related to their molecular defects. However, it is difficult to compare the abnormalities of these fibrin clots, as the reaction conditions and specimen preparation techniques for SEM analysis were different from each other.

Fibrin clot formation involves a series of highly ordered molecular interactions. Specifically, it consists of: (i) transition of fibrinogen to fibrin monomers by cleavage of FPA and B by fibrinogen-bound thrombin, (ii) construction of half-molecular overlapping double-stranded fibrin protofibrils, and (iii) lateral association of the protofibrils to form thick fibrin fibers, bundles and networks. Hereditary dysfibrinogens primarily have a functional defect in one or two of these steps, and these defects are related to the respective functional sites, FPA cleavage site, E:D binding site, D:D association site, Ca^{2+}-binding site and αC-domain. The molecular defects in the dysfibrinogens examined in the present study have been shown to be located in these sites or their vicinities. To clarify the relationships between these molecular defects and different clot structures, we conducted fibrin conversion for 38 different dysfibrinogens under the same conditions and compared the abnormalities of their fibrin clots. As a result, we were able to classify the fibrin networks into five classes. During this classification, we found two tendencies: that dysfibrinogens with slow FPA release or a defect in the E:D binding sites form normal or normal-like fibrin clots (less-ordered networks) with normal network strength toward mechanical stress, and that dysfibrinogens with a defect in the D:D association form porous A networks, in which increased fiber branching and tapering of the fibers results in shortening of the fibers. These data suggest that once the FPA is released, the fitness of the A-knob to the a-hole in the E:D binding is not strictly required and that a certain looseness can be overcome if the end-to-end D:D association proceeds normally.

In our study, the AαR16 mutant fibrins (eight AαR16C and three AαR16H), the most common dysfibrinogens with a defect in FPA release, are also classified as normal or less-ordered fibrins. The only difference between the AαR16C fibrins and

other fibrins, such as those with a defect in E:D association, is the presence of many thin fibrils entwined around the normal-like fibers at the nodes. We suppose that these thin fibrils are β-fibrin lacking FPB, as reported for the homozygous AαR16C fibrinogen Metz [14]. The extents of the thin fibrils were found to vary among the AαR16C fibrins, which is in good agreement with the variety of network structures observed, together with the slightly wider range of fiber width. We considered that this diversity could be explained from the varieties of the heterozygosis of the molecule and the chemical nature of the SH group of Aα16C residue. As normal fibrinogen is composed of two molecular halves as $(A\alpha B\beta\gamma)_2$, heterozygous AαR16C fibrinogen may exist as either two homodimers, $(A'\alpha B\beta\gamma)_2$ and normal $(A\alpha B\beta\gamma)_2$, or heterodimer $(A'\alpha B\beta\gamma\text{-}A\alpha B\beta\gamma)$ or both mixtures, although Fbg Kawaguch is composed of only homodimers [24]. Upon incubation with thrombin, three types of fibrin monomers, i.e. des-AABB fibrin monomer from normal, des-BB fibrin from homodimer and des-ABB fibrin from heterodimer would be formed. If the ratio of the homodimer to heterodimer is different in each of AαR16C dysfibrinogens, polymerization would be complicated by the multiple combinations of fibrin monomers that led to the variety of the fibrin networks. Further complication is expected from the nature of the substance that bridged by disulfide bond at Aα16C residue. As our AαR16C fibrinogens do not contain free-SH group or albumin, the Aα16C residue must have been paired with some other small substances, such as free Cys, glutathione or intermolecular disulfide bridge with the same Aα16C residue in the homodimer as we have previously shown in Fbg Kawaguchi [24]. The paired substance may interfere differently with the cleavage of FPA and B and polymerization and thus lead to the variety of the network structure among the AαR16C fibrins.

In the normal conversion to fibrin, the protofibrils are bridged intermolecularly by the αC-domain to form thick fibers [29]. However, fiber branching rarely occurs and the long fibers adhere to each other to form bundles. We further confirmed that a certain length of peptide backbone and the charged cluster in the αC-domain are necessary for this lateral association. Indeed, structural alterations involving either extra-glycosylation [17] or truncation with or without albumin attachment [16,19,30] in the αC-domain, result in the formation of two abnormal fibrins composed of highly branched thin fibers, designated porous B and lace-like networks. Lace-like networks appear to be formed by impairment of the lateral association between protofibrils, and there are no thick fibers or bundles. In the case of Fbn Marburg and Giessen, albumin bound to the αC-domain causes increased branching, similar to the case for Fbn Dusart [16]. The major difference between porous A and porous B networks are the fiber width and the numbers of tapered fiber ends, whereas the major difference between porous B and lace-like networks is the porosity of the network. All the porous B networks are easily damaged by mechanical stress, whereas the lace-like networks retain high resistance against such stress. It is notable that the network strength does not depend on the fiber width, but on the fragility which is primarily introduced by impairment of the D:D association.

We suppose that the porosity is generated during the gelation and not during preparation of SEM specimens, as we have observed many pores and irregular fiber ends in Fbn Asahi by the confocal laser scanning microscopic analysis [21]. However, the possibility of the consequence of the collapse of the networks that create tapered ends is remained in porous A fibrins. We also suppose that a fragile porous B network is formed when the D:D and lateral associations are both severely impaired, as observed in the formation of many extra carbohydrated fibrins, Fbn γM310T(CHO), AαR141S (CHO) and γA327T(CHO).

The D:D association involves binding of the D-domains of two different molecules along the same strand and is essential for the formation of a normal fibrin network. Among our observations, the extent of the impairment of the D:D association is consistent with the porosity and abnormality of the networks. When the fibrins with four different γ275 residues are compared, the sizes of the side-chains of the γ275 residue are in good agreement with the abnormality of the network. The bulky chemical constituents that exist between the D:D interface and alteration of the conformationally adjacent residues of the D:D interface may also weaken the D:D association. Considering all the above factors, we suppose that the integrity of the fibrinogen molecule is a prerequisite for the normal alignment of the two D-domains, and thus also indispensable for the regulation of fiber branching as observed in Fbg OsakaVI [20].

Failure to form hemostatic thrombi and to digest intravascular fibrin clots necessitates manifest bleeding and thrombosis, respectively. These altered functions are observed in certain types of hereditary dysfibrinogens, although half of all dysfibrinogenemia patients are asymptomatic, and are occasionally detected by coagulation studies. Alteration of the clot structure and physical properties may represent evidence that is correlated with the clinical manifestations. However, clinical manifestations should be carefully concluded, as bleeding, thrombosis or asymptomatic were reported as clinical manifestation in some dysfibrinogenemia cases with the same molecular defect such as AαR16C and AγR275C fibrinogens (see the fibrinogen data base). From our observations of 38 dysfibrinogens, we found that fibrins composed of thin fibers and classified as porous B and lace-like networks were mostly associated with either bleeding or thrombosis. On the other hand, we could not correlate the fibrins composed of normal thickness fibers with any clinical manifestations of the patients, although we found that patients who formed fibrin with a higher compaction tended to manifest bleeding or thrombosis.

As a final thought, we compared fibrin clots that were freshly prepared or from 15-year-stock dysfibrinogens, and confirmed that there were no differences among them. From these results, we conclude that the abnormality in each of the fibrin networks observed in our study is related to structural alterations arising through the molecular defect in the fibrinogen.

Acknowledgements

We thank all the doctors who collaborated with us during our studies of these dysfibrinogenemia samples. This work was supported by Grants-in-Aid for Scientific Research (14570994) from the Japanese Ministry of Education and Science; Health and Labor Science Research Grants for Research from the Japanese Ministry of Health, Labour, and Welfare; and Grants for 'High-Tech Center Research' Projects for Private Universities: matching fund subsidy from MEXT (Japanese Ministry of Education, Culture, Sports, Science and Technology), 2002–2006.

Disclosure of Conflict of Interests

The authors state that they have no conflict of interest.

References

1 Mosesson MW, Siebenlist KR, Meh DA. The structure and biological features of fibrinogen and fibrin. *Ann N Y Acad Sci* 2001; **936**: 11–30.
2 Doolittle RF, Yang Z, Mochalkin I. Crystal structure studies on fibrinogen and fibrin. *Ann N Y Acad Sci* 2001; **936**: 31–43.
3 Pratt KP, Côté HCF, Chung DW, Stenkamp RE, Davie RE. The primary fibrin polymerization pocket: three-dimensional structure of a 30-kDa C-terminal γ-chain fragment complexed with the peptide Gly-Pro-Arg-Pro. *Proc Natl Acad Sci USA* 1997; **94**: 7176–81.
4 Spraggon G, Everse SJ, Doolittle RF. Crystal structure of fragment D from human fibrinogen and its cross-linked counterpart from fibrin. *Nature* 1997; **1389**: 455–62.
5 Everse SJ, Spraggon G, Veerapandian L, Riley M, Doolittle RF. Crystal structure of fragment double-D from human fibrin with two different bound ligands. *Biochemistry* 1998; **37**: 8637–42.
6 Brown JH, Volkmann N, Jun G, Henschen-Edman AH, Cohen C. The crystal structure of modified bovine fibrinogen. *Proc Natl Acad Sci USA* 2000; **97**: 85–90.
7 Yang Z, Kollman J, Pandi L, Doolittle RF. Crystal structure of native chicken fibrinogen at 2.7 Å resolution. *Biochemistry* 2001; **40**: 12515–23.
8 Madrazo J, Brown JH, Litvinovich S, Dominguez R, Yakovlev S, Medved L, Cohen C. Crystal structure of the central region of bovine fibrinogen (E5 fragment) at 1.4-Å resolution. *Proc Natl Acad Sci USA* 2001; **98**: 11967–72.
9 Everse SJ, Spraggon G, Doolittle RF. A three-dimensional consideration of variant human fibrinogens. *Thromb Haemost* 1998; **80**: 1–9.
10 Côté HCF, Lord ST, Pratt KP. Gamma-chain dysfibrinogenemias: molecular structure-function relationships of naturally occurring mutations in the gamma chain of fibrinogen. *Blood* 1998; **92**: 2195–212.
11 Matsuda M, Sugo T. Hereditary disorders of fibrinogen. *Ann NY Acad Sci* 2001; **936**: 11–30.
12 Sugo T, Sakata Y, Matsuda M. Structural alterations in hereditary dysfibrinogens. *Curr Protein Pept Sci* 2003; **3**: 239–47.
13 Scott EM, Ariëns RA, Grant PJ. Genetic environmental determinants of fibrin structure and function: relevance to clinical disease. *Arterioscler Thromb Vasc Biol* 2004; **24**: 1558–66.
14 Mosesson MW, DiOrio PJ, Muller MF, Shainoff JR, Siebenlist KR, Amrani DL, Homandberg GA, Soria J, Soria C, Samama M. Studies on the ultrastructure of fibrin lacking fibrinopeptide B (beta-fibrin). *Blood* 1987; **69**: 1073–81.
15 Mosesson MW, Siebenlist KR, DiOrio JP, Matsuda M, Hainfeld JF, Wall JS. The role of fibrinogen D domain interaction association sites in the polymerization of fibrin and fibrinogen Tokyo II (γ275 Arg → Cys). *J Clin Invest* 1995; **96**: 1053–58.
16 Collet JP, Woodhead JL, Soria J, Soria C, Mirshahi M, Caen JP, Weisel JW. Fibrinogen Dusart: electron microscopy of molecules, fibers and clots, and viscoelastic properties of clots. *Biophys J* 1996; **70**: 500–10.
17 Woodhead JL, Nagaswami C, Matsuda M, Arocha-Piñango CL, Weisel JW. The ultrastructure of fibrinogen Caracas II molecules, fibers, and clots. *J Biol Chem* 1996; **271**: 4946–53.
18 Sugo T, Nakamikawa C, Takano H, Mimuro J, Yamaguchi S, Mosesson MW, Meh DA, DiOrio JP, Takahashi N, Takahashi H, Nagai K, Matsuda M. Fibrinogen Niigata with impaired fibrin assembly: an inherited dysfibrinogen with a Bβ Asn-160 to Ser substitution associated with extra glycosylation at Bβ Asn-158. *Blood* 1999; **94**: 3806–13.
19 DiOrio JP, Mosesson MW, Hernandez I, Sugo T, Matsuda M. Fibrinogen Marburg fibrin network structure. *Microsc Microanal* 1999; **5**: 1121–2.
20 Sugo T, Nakamikawa C, Yoshida N, Niwa K, Sameshima M, Mimuro J, Weisel JW, Nagita A, Matsuda M. End-linked homodimers in fibrinogen Osaka VI with a Bβ-chain extension lead to fragile clot structure. *Blood* 2000; **96**: 3779–85.
21 Sugo T, Sekine O, Nakamikawa C, Endo H, Arocha-Piñango CL, Matsuda M. Mode of perturbation of Asahi fibrin assembly by the extra oligosaccharides. *Ann NY Acad Sci* 2001; **936**: 223–5.
22 Marchi R, Arocha-Piñango CL, Nagy H, Matsuda M, Weisel JW. The effect of additional carbohydrate in the coiled-coil region on polymerization and clot structure and properties: characterization of the homozygous and heterozygous forms of fibrinogen Lima (Aα Arg141 Ser with extra glycosylation). *J Thromb Haemost* 2004; **2**: 940–8.
23 Hamano A, Mimuro J, Aoshima M, Ito T, Kitamura M, Nishinarita S, Takano K, Ishiwata A, Kashiwakura Y, Niwa K, Ono T, Madoiwa S, Sugo T, Matsuda M, Sakata Y. Thrombophilic dysfibrinogen Tokyo V with the amino acid substitution of γAla327Thr: formation of fragile but fibrinolysis-resistant clots and its relevance to arterial thromboembolism. *Blood* 2004; **103**: 3045–50.
24 Miyata T, Terukina S, Matsuda M, Kasamatsu A, Takeda Y, Iwanaga S. Fibrinogen Kawaguchi and Osaka: an amino acid substitution of Aα Arginine-16 to Cysteine which forms an extra interchain disulfide bridge between the two Aα chains. *J Biochem* 1987; **102**: 93–101.
25 Terukina S, Matsuda M, Hirata H, Takeda Y, Miyata T, Takao T, Shimonishi Y. Substitution of γArg-275 by Cys in an abnormal fibrinogen, "Fibrinogen Osaka II". *J Biol Chem* 1988; **263**: 13579–87.
26 Sugo T, Nakamikawa C, Takebe M, Kohno I, Egbring R, Matsuda M. Factor XIIIa cross-linking of the Marburg fibrin: formation of αm-γn heteromultimers and the α-chain-linked albumin-γ complex, and disturbed protofibril assembly resulting in acquisition of plasmin resistance relevant to thrombophila. *Blood* 1998; **91**: 3282–8.
27 Nilssen A. In Hypo-/Dysfibrinogenämie Giessen im Vergleich mit Hypo-/Dysfibrinogenämie Marburg. Doctorial dissertation. Giessen: Justus-Liebig University, 2002.
28 Yashida N, Hirata H, Morigami Y, Imaoka S, Matsuda M, Yamzumi K, Asakura S. Characterization of an abnormal fibrinogen Osaka V with the replacement of γ-Arginine 375 by Glycine. *J Biol Chem* 1992; **263**: 2753–59.
29 Veklich YI, Gorkun OV, Medved LV, Nieuwebhuizen W, Weisel JW. Carboxyl-terminal portions of the α chains of fibrinogen and fibrin. Localization by electron microscopy and the effects of isolated α fragments on polymerization. *J Biol Chem* 1993; **268**: 13577–85.
30 Marchi R, Meyer M, de Bosch N, Soria J, Arocha-Pinango CL, Weisel JW. Biophysical characterization of fibrinogen Caracas I with an Alpha-chain truncation at Aalpha-466 Ser: identification of the mutation and biophysical characterization of properties of clots from plasma and purified fibrinogen. *Blood Coagul Fibrinolysis* 2004; **15**: 285–93.

International Journal of
HEMATOLOGY

Plasminogen Activator Inhibitor 1 Promotes a Poor Prognosis in Sepsis-Induced Disseminated Intravascular Coagulation

Seiji Madoiwa,[a] Shin Nunomiya,[b] Tomoko Ono,[c] Yuichi Shintani,[c] Tsukasa Ohmori,[a] Jun Mimuro,[a] Yoichi Sakata[a]

[a]Research Division of Cell and Molecular Medicine, Center for Molecular Medicine, and [b]Division of Intensive Care, Department of Anesthesiology and Intensive Care Medicine, Jichi Medical University, Tochigi; [c]Research and Development Department, Mitsubishi Kagaku Iatron, Inc, Chiba, Japan

Received December 22, 2005; received in revised form July 24, 2006; accepted August 8, 2006

Abstract

Sepsis-induced disseminated intravascular coagulation (DIC) is a serious condition because it is closely linked to the development of multiple organ dysfunctions. We compared molecular fibrinolysis markers for 117 patients with sepsis-induced DIC and 1627 patients with nonseptic DIC. Levels of fibrinogen and fibrin degradation products and D-dimer were significantly lower in sepsis-induced DIC cases than in nonseptic DIC cases. In septic DIC cases, plasma plasminogen activator inhibitor 1 (PAI-1) levels were significantly higher than in nonseptic DIC cases. D-dimer levels were negatively correlated with plasma PAI-1 levels in septic DIC cases. Multiple Organ Dysfunction Scores were significantly higher in septic DIC patients with PAI-1 levels >90 ng/mL than in the group with PAI-1 levels <30 ng/mL. The Kaplan-Meier survival functions until 28 days after DIC diagnosis were significantly lower in the group with PAI-1 levels >90 ng/mL than in the other groups. In a multivariate analysis, plasma PAI-1 levels at DIC diagnosis were an independent risk factor for mortality in sepsis-induced DIC (hazard ratio, 1.012; $P = .008$). These data suggest that plasma PAI-1 plays an important role in sustaining DIC in septic DIC cases and contributes to multiple organ failure and decreased survival in such patients.
Int J Hematol. 2006;84:398-405. doi: 10.1532/IJH97.05190

Key words: Plasminogen activator inhibitor 1; Sepsis; Disseminated intravascular coagulation; Multiple organ failure; Prognosis

1. Introduction

Sepsis is a distressing disorder characterized by systemic activation of the inflammatory and coagulation cascades in response to microbial infection [1]. Sepsis is defined as systemic inflammatory response syndrome (SIRS) in the presence of documented or suspected infection [2], and approximately 30% of sepsis patients have combined multiple organ failure [3]. Sepsis-related organ dysfunction, which is defined as severe sepsis, has been attributed to microvascular thrombosis [4], and its mortality rate ranges from 30% to 50%, even with intensive medical treatments [5].

Disseminated intravascular coagulation (DIC) is an acquired syndrome characterized by intravascular activation of coagulation with loss of localization arising from different causes [6,7]. The clinical features of DIC include microvascular thrombotic complications that may hamper adequate blood supply to organs. In particular, DIC is widely recognized as one of the most common conditions associated with sepsis [4]. In conjunction with the hemodynamic and metabolic disorders seen in sepsis, sepsis-induced DIC might contribute to the development of multiple organ failure and result in a poor prognosis. Therefore, early diagnosis and treatment are required to improve the prognosis of sepsis-induced DIC.

The initiation of fibrinolysis is mediated by plasminogen activators and regulated by plasminogen activator inhibitor 1 (PAI-1) [8]. Besides its role in maintaining physiological

Correspondence and reprint requests: Yoichi Sakata, MD, PhD, Research Division of Cell and Molecular Medicine, Center for Molecular Medicine, School of Medicine, Jichi Medical University, 3311-1, Yakushi-ji, Shimotsuke, Tochigi 329-0498, Japan; 81-285-58-7398; fax: 81-285-44-7817 (e-mail: yoisaka@jichi.ac.jp).

Table 1.
Clinical Data for Patients with Septic and Nonseptic Disseminated Intravascular Coagulation (DIC)*

	Septic DIC	Nonseptic DIC
Cases, n	117	1627
Age, y	61.7 ± 15.4	54.8 ± 17.4
Basic disease, %		
Hematologic malignancy	—	60.6
Cancer	—	26.4
Liver disease	—	3.5
Pancreatitis	—	2.7
Trauma	—	0.9
Other noninfectious disease	—	5.8
Respiratory infection	59.6	—
GI tract or biliary tract infection	15.8	—
Urinary tract infection	10.5	—
Other infection	14.1	—
28-Day survival, %	74.4	81.5

*Age data are presented as the mean ± SD. GI indicates gastrointestinal.

hemostasis via regulating the fibrinolytic system, PAI-1 functions in many other pathophysiological processes. Suppression of the fibrinolysis system is mediated by increased plasma PAI-1 levels in DIC patients exhibiting SIRS with trauma [9]. Although there is some fibrinolytic activity in response to the formation of fibrin, the level of this activity is too low to counteract the systemic deposition of fibrin in SIRS [10]. In fact, high levels of PAI-1 have been reported to predict an adverse outcome in severe sepsis, and suppressed fibrinolysis is believed to be one of the most important predictors of multiple organ dysfunction during DIC [11,12]. However, it has not been clarified whether plasma PAI-1 levels are independent predictors of mortality or are merely a surrogate for the multiple organ dysfunction score in septic DIC cases.

In this study, we evaluated molecular markers with multivariate analysis, and by evaluating molecular markers for fibrinolysis in patients with sepsis-induced DIC, we have shown that plasma PAI-1 plays an important role in determining the prognosis in sepsis-induced DIC.

2. Materials and Methods

2.1. Study Population

We examined hemostatic abnormalities in 4797 patients suspected of having associated DIC. Diagnoses of the presence of DIC in 1744 of these cases were made in accordance with a modified version of the criteria established by the Japanese Ministry of Health and Welfare [13]. In brief, the basic disorder, the clinical conditions (ie, bleeding symptoms and organ dysfunction), and the results of the examination (ie, platelet counts, prothrombin time, fibrinogen, and fibrinogen and fibrin degradation products [FDPs]) were quantified on a score basis (maximum = 13; minimum = 0). If the number was ≥7, DIC was established. We identified 117 cases with septic DIC and 1627 cases with nonseptic DIC and collected the baseline characteristics of the patients, including demographic information, Multiple Organ Dysfunction Scores using the Sequential Organ Failure Assessment score [14], site and type of infection, and hematologic test results.

The diagnosis of sepsis was made according to the guidelines of the definition of the American College of Chest Physicians/Society of Critical Care Medicine Consensus Conference [15]. In brief, patients had to meet at least 3 of the 4 criteria for a systemic inflammatory response and had to have a known or suspected infection, as evidenced by one or more of the following: presence of bacteremia, pathologic microorganisms or white blood cells in a normally sterile body fluid such as urine and joint fluid, the production of purulent sputum, radiographic evidence of pneumonia, clinical signs associated with a high risk of infection (eg, cholangitis, peritonitis), or increased levels of endotoxin, β-D-glucan, or *Candida* antigen.

2.2. Blood Samples and Quantification of Molecular Markers of DIC

All samples were obtained with informed consent from patients according to the Declaration of Helsinki. Citrated plasma and serum samples were stored at –80°C until analyzed. The prothrombin time and the activated partial thromboplastin time were measured with coagulation-based activity assays. Plasma fibrinogen levels were measured by clotting methods using Fibrinogen Test Sankyo (Sankyo, Tokyo, Japan). FDP levels in sera were determined by the latex

Table 2.
Characterization of Bacterial Pathogen and Sequential Organ Failure Assessment (SOFA) Score for Patients with Sepsis-Induced Disseminated Intravascular Coagulation (n = 117)

Positive blood culture, %	37.8
Results of Gram staining for bacterial pathogen, %	
Purely Gram-positive	36.5
Purely Gram-negative	28.5
Mixed	9.5
Culture negative or not obtained	25.3
Type of organism, %	
Gram-positive	
Staphylococcus aureus	44.6
Other *Staphylococcus* species	3.5
Streptococcus pneumoniae	5.4
Other Gram-positive species	1.7
Gram-negative	
Escherichia coli	7.1
Klebsiella species	7.1
Pseudomonas species	16.1
Other Gram-negative species	10.5
Fungus, %	3.5
SOFA score*	
Gram-positive infection	6.1 ± 4.3
Gram-negative infection	7.2 ± 2.3

*Data are presented as the mean ± SD. The difference between SOFA scores is not statistically significant.

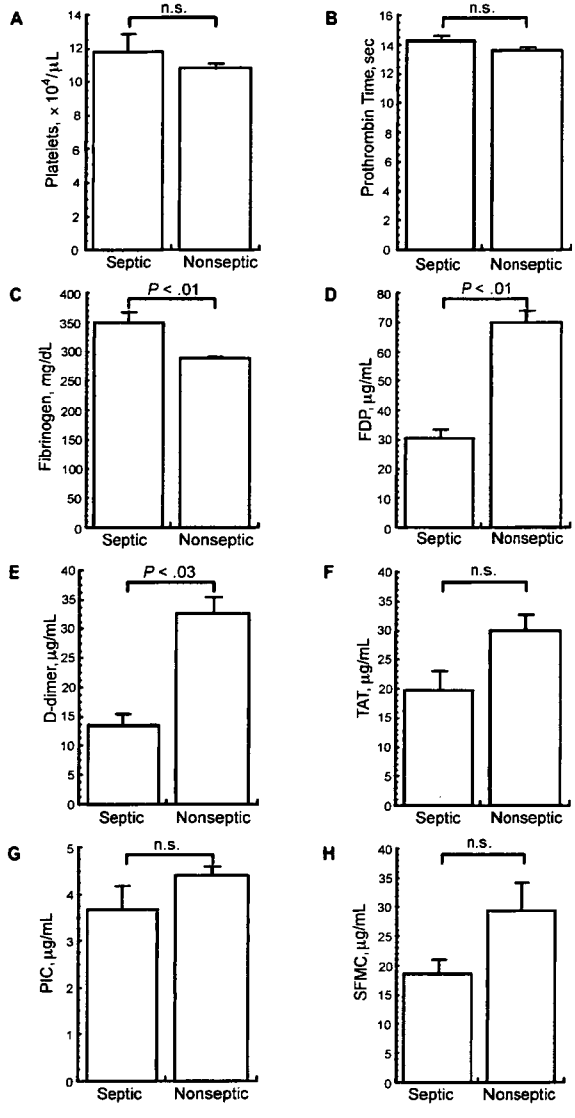

Figure 1. The levels of molecular markers for the fibrinolysis system are lower in septic disseminated intravascular coagulation (DIC) cases than in nonseptic DIC cases. The following fibrinolytic parameters were measured as described in "Materials and Methods" in DIC cases with or without sepsis: platelet counts (A), prothrombin time (B), fibrinogen (C), fibrinogen and fibrin degradation products (FDP) (D), D-dimer (E), thrombin–antithrombin III complex (TAT) (F), plasmin–α_2-plasmin inhibitor complex (PIC) (G), soluble fibrin monomer complex (SFMC) (H). Data are presented as the mean ± SEM. NS indicates not statistically significant.

agglutination assay using LPIA-FDP (Mitsubishi Kagaku Iatron, Tokyo, Japan). Plasma D-dimer and plasmin–α_2-plasmin inhibitor complex (PIC) levels were measured by enzyme-linked immunosorbent assay (ELISA) (Kokusai-Shiyaku, Kobe, Japan). Plasma levels of thrombin–antithrombin III complexes were quantified by ELISA (Sysmex, Kobe, Japan). Soluble fibrin monomer complex (SFMC) levels were also determined by the latex agglutination assay and using monoclonal antibody IF-43 [16]. For the PAI-1 assay, we used a latex photometric immunoassay (LPIA-200; Mitsubishi Chemical, Tokyo, Japan), as previously described [17].

2.3. Statistical Analysis

The SPSS statistical software package (SPSS, Chicago, IL, USA) was used for the statistical calculations of all data analyses. Normally distributed variables were presented as the mean ± SEM and compared by means of the Student *t* test or 1-way analysis of variance. Variables not normally distributed were analyzed with the 2-sided Mann-Whitney *U* test. A difference with $P < .05$ was considered statistically significant. Multivariate logistic regression analyses were used to identify independent predictors of mortality in septic DIC cases. Kaplan-Meier product limits were computed for the freedom from endpoint, and the log-rank test was used for screening univariate group results regarding the outcomes. Multivariate Cox regression models were used to investigate the association of plasma PAI-1 levels with the 28-day mortality rate after DIC diagnosis.

3. Results

3.1. Gram-Negative Septic DIC Patients and Gram-Positive Septic DIC Patients Showed Similar Severities of Organ Failures

The baseline characteristics of our patients are summarized in Table 1. We found no significant difference in the 28-day survival rate between the septic DIC and nonseptic DIC groups. The blood cultures from 37.8% of the patients with septic DIC showed positive Gram staining (Table 2). Those with a purely Gram-positive bacterial infection comprised 36.5% of the patients, and those with a purely Gram-negative infection comprised 28.5%. *Staphylococcus aureus* was the microbe most frequently isolated from patients with Gram-positive bacterial DIC. This result may indicate that the patient population with an immunosuppressed state, such as those undergoing chemotherapy, might affect the characterization of bacterial pathogens in our septic DIC cases. On the other hand, *Pseudomonas aeruginosa* was the most frequent causative agent in septic DIC cases with Gram-negative bacterial infection. We analyzed the Multiple Organ Dysfunction Scores of the sepsis-induced DIC cases and found that Gram-positive septic DIC patients had scores similar to those of Gram-negative DIC patients (Table 2).

3.2. Levels of Molecular Markers for the Fibrinolysis System Were Lower in Septic DIC Cases than in Nonseptic DIC Cases

There were no significant differences in platelet numbers and prothrombin times between sepsis-induced DIC and nonseptic DIC patients (Figures 1A and 1B). The sepsis-induced DIC patients had markedly higher levels of plasma fibrinogen than nonseptic DIC patients (Figure 1C). In contrast, FDP and D-dimer levels in septic DIC cases were significantly lower than the respective levels in nonseptic DIC cases ($P < .01$, and $P < .03$, respectively; Figures 1D and 1E).

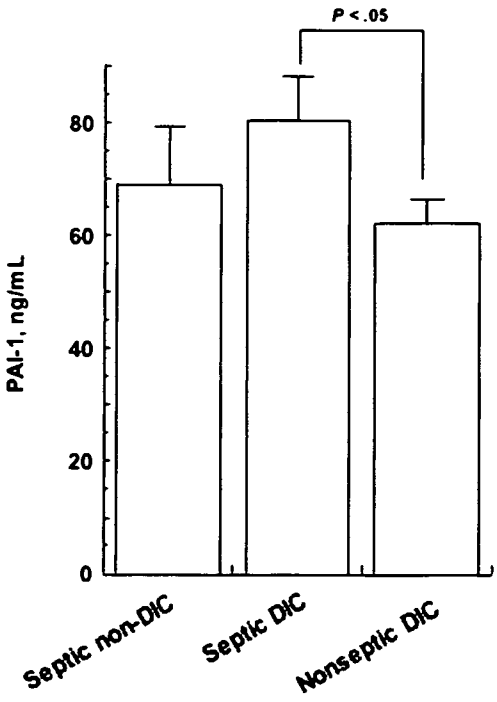

Figure 2. Plasma plasminogen activator inhibitor 1 (PAI-1) levels are increased in septic disseminated intravascular coagulation (DIC) cases. Plasma PAI-1 levels in septic non-DIC, septic DIC, and nonseptic DIC patients were measured as described in "Materials and Methods." Data are presented as the mean ± SEM.

3.3. PAI-1 Suppresses the Fibrinolysis System in Sepsis-Induced DIC Cases

We compared the plasma PAI-1 levels of septic non-DIC patients (69.03 ± 10.2 ng/mL, n = 78) with those of septic DIC and nonseptic DIC patients. The PAI-1 levels of septic non-DIC patients were nonsignificantly lower than those of septic DIC patients, and there were no statistical differences between the PAI-1 levels of septic non-DIC cases and those of nonseptic DIC cases. However, the PAI-1 levels of septic DIC cases were significantly higher than those of nonseptic DIC cases (80.23 ± 7.96 ng/mL versus 62.01 ± 4.42 ng/mL, $P = .046$) (Figure 2). It is known that PAI-1 is proteolytically cleaved and its concentration is decreased in patients with acute promyelocytic leukemia (APL)-induced DIC [18], so we excluded 111 APL cases from the nonseptic DIC group and compared PAI-1 levels for the septic DIC cases and the nonseptic DIC cases without APL. The plasma PAI-1 levels of the septic DIC cases were significantly higher than those of the nonseptic, non-APL DIC cases (80.23 ± 7.96 versus 62.72 ± 4.53 ng/mL, $P < .05$). To address whether the down-regulation of the fibrinolysis system is caused by increased levels of PAI-1 in septic DIC patients, we studied the relationship between plasma PAI-1 and D-dimer levels. When the patients with sepsis-induced DIC were classified into 4 groups according to PAI-1 levels, plasma fibrinogen levels were significantly increased in the groups with PAI-1 levels of 30 to 60 ng/mL, 60 to 90 ng/mL, and greater than 90 ng/mL, compared with the fibrinogen levels in the group with PAI-1 levels of less than 30 ng/mL ($P < .03$, $P < .05$, and

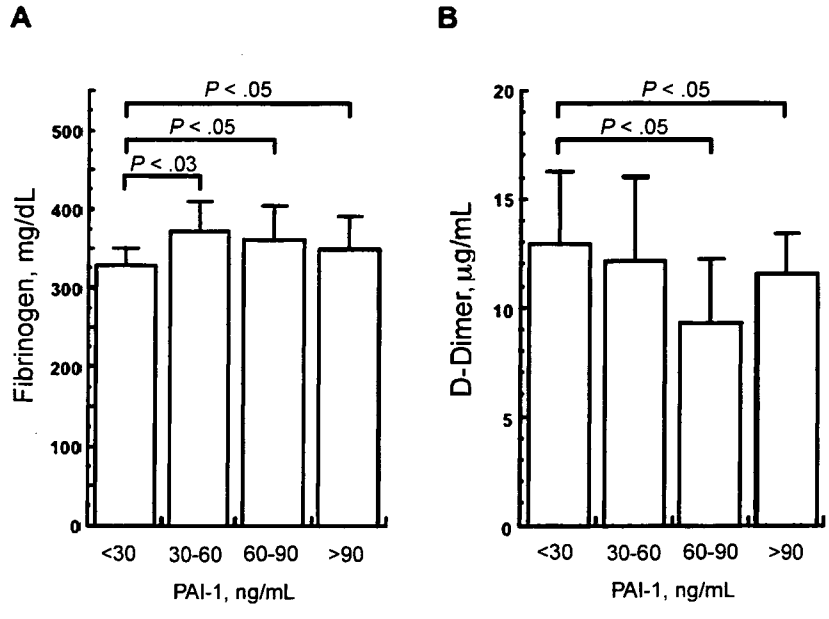

Figure 3. Relationship between plasma plasminogen activator inhibitor 1 (PAI-1) level and plasma fibrinogen or D-dimer level in sepsis-induced disseminated intravascular coagulation (DIC) cases. DIC patients were classified into 4 groups according to PAI-1 level (<30 ng/mL [n = 33], 30-60 ng/mL [n = 33], 60-90 ng/mL [n = 21], and >90 ng/mL [n = 30]), and the groups were compared with respect to plasma fibrinogen (A) and D-dimer (B) levels. Data are presented as the mean ± SEM.

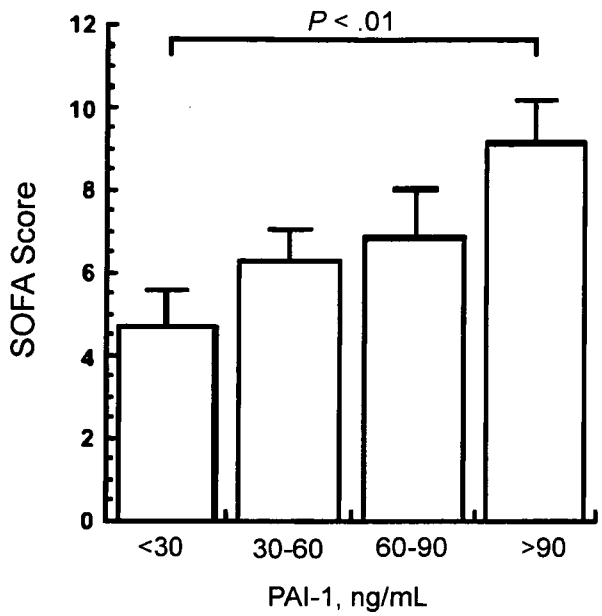

Figure 4. Plasma plasminogen activator inhibitor 1 (PAI-1) levels correlate with Multiple Organ Dysfunction Scores using the Sequential Organ Failure Assessment (SOFA) score in cases of septic disseminated intravascular coagulation (DIC). DIC patients were classified into 4 groups according to PAI-1 level at the time of DIC diagnosis (<30 ng/mL [n = 33], 30-60 ng/mL [n = 33], 60-90 ng/mL [n = 21], and >90 ng/mL [n = 30]), and the groups were compared with respect to SOFA scores. Data are presented as the mean ± SEM.

$P < .05$, respectively; Figure 3A). In contrast, D-dimer levels in the groups with PAI-1 levels of 60 to 90 ng/mL and greater than 90 ng/mL were significantly lower than those in the group with PAI-1 levels of less than 30 ng/mL (Figure 3B).

3.4. Plasma PAI-1 Levels Correlated with Multiple Organ Failure and a Negative Prognosis in Sepsis-Induced DIC Cases

When we compared the relationship between plasma PAI-1 levels and the Multiple Organ Dysfunction Scores in sepsis-induced DIC cases, we found that these scores were significantly higher in the group with PAI-1 levels greater than 90 ng/mL than in the group with PAI-1 levels less than 30 ng/mL (4.7 points versus 9.1 points, $P < .01$; Figure 4). In septic non-DIC cases, the Kaplan-Meier survival functions in the group with PAI-1 levels greater than 90 ng/mL were not significantly lower than those of the groups with levels of 30 to 60 ng/mL and 60 to 90 ng/mL (Figure 5A). In contrast, the survival rate until 28 days after DIC diagnosis in the group with PAI-1 levels greater than 90 ng/mL was significantly lower than the rates in the groups with PAI-1 levels of less than 30 ng/mL, 30 to 60 ng/mL, and 60 to 90 ng/mL ($P < .01$ for all 3 tests; Figure 5B). Cox regression analyses of time-to-event among patients according to plasma PAI-1 levels at the time of DIC diagnosis revealed that the adjusted odds for the 28-day mortality rate in the group with PAI-1 levels greater than 90 ng/mL (hazard ratio, 23.433; 95% confidence interval, 3.00-182.84 [$P = .003$]; Table 3) were significantly higher than those in the other groups. Plasma PAI-1 level seemed to be an independent risk factor for mortality in the multivariate logistic regression analyses of molecular markers in sepsis-induced DIC cases (hazard ratio, 1.012; 95% confidence interval, 1.003-1.020 [$P = .008$]; Table 4), although platelet and FDP levels might also affect the mortality. These data indicate that plasma PAI-1 levels at the time of DIC diagnosis could serve as an important index for prognostic assessment in sepsis-induced DIC cases.

4. Discussion

DIC is currently accepted to be a pathologic state that occurs acutely over the course of a severe underlying disease, such as sepsis, and is indicated by the presence of hemorrhagic symptoms, multiple organ failure, and/or occasional thrombotic complications [19]. We observed that 37.8% of

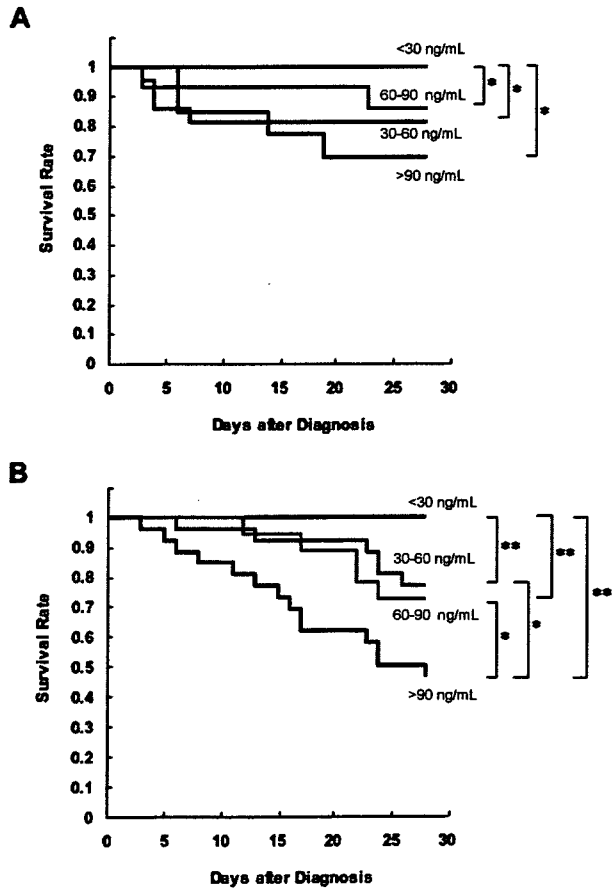

Figure 5. Plasma plasminogen activator inhibitor 1 (PAI-1) levels correlate with the mortality rate by 28 days after diagnosis in septic disseminated intravascular coagulation (DIC) cases. A, Kaplan-Meier plots with respect to plasma PAI-1 level (<30 ng/mL [n = 33], 30-60 ng/mL [n = 33], 60-90 ng/mL [n = 21], and >90 ng/mL [n = 30]) for septic non-DIC patients. B, Kaplan-Meier plots with respect to the same plasma PAI-1 levels at the time of DIC diagnosis for sepsis-induced DIC patients. *$P < .05$; **$P < .03$.

Table 3.
Cox Regression Analyses of Time-to-Event among Patients according to Plasminogen Activator Inhibitor 1 (PAI-1) Level at Diagnosis of Sepsis-Induced Disseminated Intravascular Coagulation (DIC) (n = 117)*

	28-Day Mortality after DIC Diagnosis	
PAI-1, ng/mL	Hazard Ratio (95% CI)	*P*
<30	1.000	—
30-60	8.183 (0.941-71.171)	.057
60-90	9.088 (1.053-78.406)	.045
>90	23.433 (3.003-182.844)	.003

*CI indicates confidence interval.

septic DIC patients show blood cultures positive for bacterial infection (Table 2). These results are compatible with previous studies that showed accepted proof of serious infection [20-22]. Experimental studies based on models of Gram-negative sepsis have shown that DIC characteristically exhibits strongly enhanced inflammatory activity, activated coagulation, and impaired fibrinolysis [23,24]. In contrast, Gram-positive bacteria are reportedly the predominant pathogens of sepsis [25], and they can cause septic shock and multiple organ failure without causing endotoxemia [26]. The severity of multiple organ failure in Gram-positive DIC patients was similar to that in Gram-negative septic DIC patients (Table 2). Taken together, our data indicate that it may be difficult to predict the severity of septic DIC by the causative microorganisms isolated from patient specimens.

Because DIC is essentially a diagnosis based on laboratory data, which are obtained by different means, several combinations of these tools have been used to estimate its prevalence. We observed no significant differences in platelet numbers between sepsis-induced DIC and nonseptic DIC patients (Figure 1A). In addition, the levels of thrombin–antithrombin III complex (Figure 1F) and SFMC for these groups were not significantly different (Figure 1H). However, when we compared the SFMC levels of septic DIC cases and APL-based nonseptic DIC cases, we found that the SFMC levels of nonseptic DIC patients with APL were significantly higher than those of septic DIC patients (29.9 ± 3.7 μg/mL versus 18.6 ± 2.4 μg/mL, $P < .03$). These data are compatible with a previous report that plasma levels of soluble fibrin monomer were increased in patients with APL [27]. Thus, the activation of blood coagulation is a hallmark of DIC, and septic and nonseptic DIC cases appear to be similar in the degree of this activation. In contrast, concentrations of molecular markers for fibrinolysis, such as FDPs and D-dimer in septic DIC cases, were significantly lower than those in nonseptic DIC cases (Figure 1D and Figure 1E, respectively), suggesting that septic DIC patients are characterized by coagulation activation and the inhibition of fibrinolysis. PIC levels were nonsignificantly lower in septic DIC cases (3.6 ± 0.4 μg/mL) than in nonseptic DIC cases (4.4 ± 0.1 μg/mL, $P = .056$). Plasma PIC levels at the onset of DIC are reportedly decreased compared with the levels before the onset of DIC in nonleukemic DIC cases [28]. In addition, plasma PIC levels have been demonstrated to increase at the initial onset of hematologic malignancy but not during its relapse [27]. Patients with nonhematologic malignancy and relapsed leukemic cases were included in our study, and these subgroups might have affected the PIC levels for the nonseptic DIC cases. However, further prospective studies are necessary to clarify whether the plasma PIC levels of septic and nonseptic DIC cases are different.

To address how the fibrinolysis system is suppressed in septic DIC patients, we compared plasma PAI-1 levels for septic and nonseptic DIC cases, because PAI-1 is a specific inhibitor of plasminogen activator and is the most important physiological regulator controlling the initial stage of the fibrinolysis system [8]. As is shown in Figure 2, plasma PAI-1 levels were significantly higher in septic DIC patients than in nonseptic DIC patients. The decreased fibrinolytic activity in healthy subjects given endotoxin is well known to be mainly due to the appearance of PAI-1 [29,30]. We showed that D-dimer levels were significantly lower in the groups with PAI-1 levels of 60 to 90 ng/mL and greater than 90 ng/mL than in those in the group with PAI-1 levels less than 30 ng/mL (Figure 3B). The plasma PAI-1 levels of septic DIC patients were positively correlated with fibrinogen levels, which were significantly higher in septic DIC patients than in nonseptic DIC patients (Figures 1C and 3A). Both PAI-1 and fibrinogen are known to be up-regulated as part of the systemic acute-phase response including sepsis [31-34]. Therefore, in septic DIC, fibrinogen could be abundantly supplied into the plasma milieu as a substrate for thrombin, and the retardation of clot lysis might be induced by the elevated PAI-1 level [31], causing imbalances between coagulation and the fibrinolysis system.

Multiple Organ Dysfunction Scores have been shown to be useful for evaluating organ failure in multicenter trials [14] and reportedly are a useful scoring system for predicting the outcome of DIC patients in the intensive care unit [35]. In sepsis-induced DIC patients, the Multiple Organ Dysfunction Scores in the group with PAI-1 levels greater than 90 ng/mL were significantly higher than those in the group with PAI-1 levels less than 30 ng/mL (Figure 4). In addition, low FDP levels have been reported to function as markers of aggravating diseases in DIC cases [12]. These results facilitated our evaluation of whether initial PAI-1 levels not only correlate with Multiple Organ Dysfunction Scores but also

Table 4.
Logistic Regression Analyses of Molecular Markers for 28-Day Mortality after Diagnosis of Sepsis-Induced Disseminated Intravascular Coagulation (DIC) (n = 117)*

	28-Day Mortality after DIC Diagnosis	
	Hazard Ratio (95% CI)	*P*
Platelets, $\times 10^3/\mu L$	0.909 (0.835-0.984)	.019
Prothrombin time, s	1.112 (0.969-1.276)	.131
Fibrinogen, mg/dL	0.999 (0.996-1.003)	.666
FDP, μg/mL	1.039 (1.002-1.078)	.040
D-dimer, μg/mL	0.976 (0.914-1.042)	.460
TAT, ng/mL	0.998 (0.982-1.015)	.840
PIC, μg/mL	0.829 (0.656-1.048)	.118
PAI-1, ng/mL	1.012 (1.003-1.020)	.008

*CI indicates confidence interval; FDP, fibrinogen and fibrin degradation products; TAT, thrombin–antithrombin III complex; PIC, plasmin–α_2-plasmin inhibitor complex; PAI-1, plasminogen activator inhibitor 1.

predict the prognosis of sepsis-induced DIC. Thus, PAI-1 may contribute to the development of organ failure by inhibiting microthrombus dissolution in septic DIC patients. Leithauser et al reported that none of the hemostatic parameters were associated with multiple organ failure at the onset of sepsis [36]. In contrast, PAI-1 has been shown to be a good prognostic marker in patients with septic shock and post-trauma DIC [9,33]. Septic DIC is not a pathologic condition similar to sepsis accompanied by multiple organ failure, because septic DIC is defined as "overt coagulation disorder" based on infection [37]. To our knowledge, there has been no study of whether plasma PAI-1 levels are independent predictors of prognosis or merely a surrogate for the Multiple Organ Dysfunction Score in septic DIC. We showed by Kaplan-Meier analyses that the rates of survival until 28 days after DIC diagnosis were significantly lower in the group with PAI-1 levels greater than 90 ng/mL, compared with other groups (Figure 5B). Moreover, plasma PAI-1 level was an independent risk factor for 28-day mortality according to multivariate logistic regression analyses (Table 4). It remains important to investigate new markers as potential predictors of poor prognosis during the early stage of sepsis-induced DIC. However, our results imply that PAI-1 plays an important role in the onset of organ dysfunction, making the prognosis of septic DIC patients unfavorable.

Acknowledgments

This work was supported in part by a Health and Labor Sciences Research Grant for Research from the Ministry of Health, Labor, and Welfare, and by a grant from the High-Tech Research Center Project for Private Universities: matching fund subsidy from the Japanese Ministry of Education, Culture, Sports, Science, and Technology, 2002-2006. We thank Ms. Chizuko Nakamikawa and Miyuki Tezuka for their excellent technical assistance. We also thank Dr. Stephanie Jung (Kurume Universities, Kurume, Japan) for the critical reading and editing of this manuscript.

References

1. Wheeler AP, Bernard GR. Treating patients with severe sepsis. *N Engl J Med.* 1999;340:207-214.
2. Bone RC, Sibbald WJ, Sprung CL. The ACCP-SCCM consensus conference on sepsis and organ failure. *Chest.* 1992;101:1481-1483.
3. Thijs LG, de Boer JP, de Groot MC, Hack CE. Coagulation disorders in septic shock. *Intensive Care Med.* 1993;19(suppl 1):S8-S15.
4. Levi M, ten Cate H. Disseminated intravascular coagulation. *N Engl J Med.* 1999;341:586-592.
5. Rangel-Frausto MS, Pittet D, Costigan M, Hwang T, Davis CS, Wenzel RP. The natural history of the systemic inflammatory response syndrome (SIRS): a prospective study. *JAMA.* 1995;273:117-123.
6. Baker WF Jr. Clinical aspects of disseminated intravascular coagulation: a clinician's point of view. *Semin Thromb Hemost.* 1989;15:1-57.
7. Taylor FB Jr, Toh CH, Hoots WK, Wada H, Levi M, for the Scientific Subcommittee on Disseminated Intravascular Coagulation (DIC) of the International Society on Thrombosis and Haemostasis (ISYH). Towards definition, clinical and laboratory criteria, and a scoring system for disseminated intravascular coagulation. *Thromb Haemost.* 2001;86:1327-1330.
8. Sprengers ED, Kluft C. Plasminogen activator inhibitors. *Blood.* 1987;69:381-387.
9. Gando S, Nakanishi Y, Tedo I. Cytokines and plasminogen activator inhibitor-1 in posttrauma disseminated intravascular coagulation: relationship to multiple organ dysfunction syndrome. *Crit Care Med.* 1995;23:1835-1842.
10. Gando S, Kameue T, Nanzaki S, Nakanishi Y. Disseminated intravascular coagulation is a frequent complication of systemic inflammatory response syndrome. *Thromb Haemost.* 1996; 75:224-228.
11. Mesters RM, Florke N, Ostermann H, Kienast J. Increase of plasminogen activator inhibitor levels predicts outcome of leukocytopenic patients with sepsis. *Thromb Haemost.* 1996;75:902-907.
12. Asakura H, Ontachi Y, Mizutani T, et al. An enhanced fibrinolysis prevents the development of multiple organ failure in disseminated intravascular coagulation in spite of much activation of blood coagulation. *Crit Care Med.* 2001;29:1164-1168.
13. Kobayashi N, Maekawa T, Takada M, Tanaka H, Gonmori H. Criteria for diagnosis of DIC based on the analysis of clinical and laboratory findings in 345 DIC patients collected by the Research Committee on DIC in Japan. *Bibl Haematol.* 1983:265-275.
14. Vincent JL, de Mendonca A, Cantraine F, et al. Use of the SOFA score to assess the incidence of organ dysfunction/failure in intensive care units: results of a multicenter, prospective study. Working Group on "Sepsis-Related Problems" of the European Society of Intensive Care Medicine. *Crit Care Med.* 1998;26:1793-1800.
15. American College of Chest Physicians/Society of Critical Care Medicine Consensus Conference. Definitions for sepsis and organ failure and guidelines for the use of innovative therapies in sepsis. *Crit Care Med.* 1992;20:864-874.
16. Soe G, Kohno I, Inuzuka K, Itoh Y, Matsuda M. A monoclonal antibody that recognizes a neo-antigen exposed in the E domain of fibrin monomer complexed with fibrinogen or its derivatives: its application to the measurement of soluble fibrin in plasma. *Blood.* 1996;88:2109-2117.
17. Ono T, Sogabe M, Ogura M, Furusaki F. Automated latex photometric immunoassay for total plasminogen activator inhibitor-1 in plasma. *Clin Chem.* 2003;49:987-989.
18. Sakata Y, Murakami T, Noro A, Mori K, Matsuda M. The specific activity of plasminogen activator inhibitor-1 in disseminated intravascular coagulation with acute promyelocytic leukemia. *Blood.* 1991;77:1949-1957.
19. Slofstra SH, Spek CA, ten Cate H. Disseminated intravascular coagulation. *Hematol J.* 2003;4:295-302.
20. Bernard GR, Wheeler AP, Russell JA, et al, for the Ibuprofen in Sepsis Study Group. The effects of ibuprofen on the physiology and survival of patients with sepsis. *N Engl J Med.* 1997;336:912-918.
21. Kieft H, Hoepelman AI, Zhou W, Rozenberg-Arska M, Struyvenberg A, Verhoef J. The sepsis syndrome in a Dutch university hospital: clinical observations. *Arch Intern Med.* 1993;153:2241-2247.
22. Opal SM, Fisher CJ Jr, Dhainaut JF, et al. Confirmatory interleukin-1 receptor antagonist trial in severe sepsis: a phase III, randomized, double-blind, placebo-controlled, multicenter trial. The Interleukin-1 Receptor Antagonist Sepsis Investigator Group. *Crit Care Med.* 1997;25:1115-1124.
23. Jansen PM, Eisele B, de Jong IW, et al. Effect of C1 inhibitor on inflammatory and physiologic response patterns in primates suffering from lethal septic shock. *J Immunol.* 1998;160:475-484.
24. Welty-Wolf KE, Carraway MS, Miller DL, et al. Coagulation blockade prevents sepsis-induced respiratory and renal failure in baboons. *Am J Respir Crit Care Med.* 2001;164:1988-1996.
25. Martin GS, Mannino DM, Eaton S, Moss M. The epidemiology of sepsis in the United States from 1979 through 2000. *N Engl J Med.* 2003;348:1546-1554.
26. Wakabayashi G, Gelfand JA, Jung WK, Connolly RJ, Burke JF, Dinarello CA. *Staphylococcus epidermidis* induces complement activation, tumor necrosis factor and interleukin-1, a shock-like state and tissue injury in rabbits without endotoxemia: comparison to *Escherichia coli*. *J Clin Invest.* 1991;87:1925-1935.
27. Nakasaki T, Wada H, Mori Y, et al. Decreased tissue factor and tissue-plasminogen activator antigen in relapsed acute promyelocytic leukemia. *Am J Hematol.* 2000;64:145-150.

28. Wada H, Sakuragawa N, Mori Y, et al. Hemostatic molecular markers before the onset of disseminated intravascular coagulation. *Am J Hematol.* 1999;60:273-278.
29. Suffredini AF, Harpel PC, Parrillo JE. Promotion and subsequent inhibition of plasminogen activation after administration of intravenous endotoxin to normal subjects. *N Engl J Med.* 1989; 320:1165-1172.
30. Levi M, ten Cate H, van der Poll T, van Deventer SJ. Pathogenesis of disseminated intravascular coagulation in sepsis. *JAMA.* 1993;270:975-979.
31. Colucci M, Paramo JA, Collen D. Generation in plasma of a fast-acting inhibitor of plasminogen activator in response to endotoxin stimulation. *J Clin Invest.* 1985;75:818-824.
32. Paramo JA, Fernandez Diaz FJ, Rocha E. Plasminogen activator inhibitor activity in bacterial infection. *Thromb Haemost.* 1988;59:451-454.
33. Pralong G, Calandra T, Glauser MP, et al. Plasminogen activator inhibitor 1: a new prognostic marker in septic shock. *Thromb Haemost.* 1989;61:459-462.
34. Otto JM, Grenett HE, Fuller GM. The coordinated regulation of fibrinogen gene transcription by hepatocyte-stimulating factor and dexamethasone. *J Cell Biol.* 1987;105:1067-1072.
35. Okabayashi K, Wada H, Ohta S, Shiku H, Nobori T, Maruyama K. Hemostatic markers and the sepsis-related organ failure assessment score in patients with disseminated intravascular coagulation in an intensive care unit. *Am J Hematol.* 2004;76:225-229.
36. Leithauser B, Matthias FR, Nicolai U, Voss R. Hemostatic abnormalities and the severity of illness in patients at the onset of clinically defined sepsis: possible indication of the degree of endothelial cell activation? *Intensive Care Med.* 1996;22:631-636.
37. Dempfle CE. Coagulopathy of sepsis. *Thromb Haemost.* 2004;91:213-224.

HUMAN GENE THERAPY 17:921–928 (September 2006)

Adipose Tissue as a Novel Target for *In Vivo* Gene Transfer by Adeno-Associated Viral Vectors

HIROAKI MIZUKAMI,[1] JUN MIMURO,[2] TSUYOSHI OGURA,[1] TAKASHI OKADA,[1] MASASHI URABE,[1] AKIHIRO KUME,[1] YOICHI SAKATA,[2] and KEIYA OZAWA[1]

ABSTRACT

Traditionally, skeletal muscle and liver are the preferred target organs for gene transfer to supply a transgene product into the systemic circulation. In this respect, adipose tissue presents a number of attractive features. However, adipose tissue transduction *in vivo* has not been feasible by conventional methods. To solve this issue, we tested the utility of excipients in adeno-associated virus (AAV) vector-mediated gene transfer and found that Pluronics are suitable for this purpose. In a histological analysis of adipose tissue in *db/db* mice, Pluronic F88 showed the greatest augmentative effect on β-galactosidase expression in combination with the AAV1 vector. When the vector encoding mouse erythropoietin (Epo) was used in the same manner, increased plasma Epo concentrations were observed (230 ± 80 versus 58 ± 14 mU/ml). Moreover, the plasma Epo concentration returned to the normal level after the surgical removal of transduced adipose tissue. No damage was observed in the transduced tissue. Our results indicate that the proposed method is safe and efficient for gene transfer into adipose tissues, thus providing an alternative for supplemental gene therapy.

OVERVIEW SUMMARY

Adipose tissue holds promise as an alternative depot organ in gene transfer approaches. However, no efficient method of gene transfer into adipose tissue *in vivo* has been established. In this study, we explored the utility of excipients to augment gene transfer into the adipose tissue of mice and found that Pluronic F88 was useful for this purpose when combined with AAV serotype 1 vectors. The improvement was also demonstrated with vectors encoding murine erythropoietin, and the mice became polycythemic. Moreover, after removing transduced adipose tissue, plasma erythropoietin levels returned to normal, which suggests the unique advantage of this method.

INTRODUCTION

In supplemental gene therapy, skeletal muscle and the liver have been the preferred targets for gene transfer to supply transgene products into the systemic circulation. However, adipose tissue presents a number of attractive features. Adipose tissue can be found throughout the body and is easily accessible for vector injection. Increasing evidence supports the notion that adipocytes are designed to secrete numerous factors into the systemic circulation (Mohamed-Ali *et al.*, 1998). Further, the majority of adipocytes are considered to be nondividing, which is suitable for achieving long-term expression of transferred genes by the use of nonintegrating vectors such as adeno-associated virus (AAV) vectors (Russell and Kay, 1999). Moreover, the transduced tissue can be safely removed when unexpected events occur, thus adding a unique feature to safety considerations. However, adipose tissue transduction has not been feasible through conventional methods, and few studies have investigated its efficacy *in vivo* (Nagamatsu *et al.*, 2001; Ogata *et al.*, 2004). To overcome these limitations and develop a more practical method, we tested the usefulness of excipients for gene transfer. To achieve efficient and widespread gene transfer, it is essential to assure that the vectors stay within the target tissue for a certain period of time. For this purpose, nonionic surfactants are promising because they have low toxicity and unique features that help stabilize the membrane (American Pharmaceutical Association [AphA] and Royal Pharmaceutical Society of Great Britain [RPSGB], 1986). Moreover,

[1]Division of Genetic Therapeutics and [2]Division of Cell and Molecular Medicine, Center for Molecular Medicine, Jichi Medical University, Tochigi 329-0498, Japan.

improved gene delivery with Pluronic compounds was demonstrated in various applications (Kabanov and Alakhov, 2002; Kabanov *et al.*, 2005). Therefore, we tested the effects of these compounds on *in vivo* gene transfer targeting adipose tissue.

MATERIALS AND METHODS

Cells and plasmids for AAV vector preparation

HEK293 cells, a human embryonic kidney cell line, were maintained as described in a previous report (Fan *et al.*, 1998). Murine erythropoietin (Epo)-encoding plasmids have already been described by Mochizuki *et al.* (2004). AAV vectors of serotype 1 through 5, which encode LacZ or Epo and have a cytomegalovirus (CMV) promoter, were prepared by transient transfection, purified and quantitated as described previously (Matsushita *et al.*, 1998; Mochizuki *et al.*, 2004). Usually, the stocks of AAV vectors contained approximately 1-2 $\times$ 10^{10} genome copies/μl.

In vitro *assessment of potential toxicity of surfactants*

A panel of Pluronics was provided by Asahi Denka (Tokyo, Japan). Tween 80 was obtained from Sigma-Aldrich (St. Louis, MO). The surfactants were dissolved in distilled H_2O to prepare stock solutions at a concentration of 20%. To assess the potential compatibility, we added various concentrations of these surfactants to cultured 293 cells at the time of confluency. After 24 hr, the cells were examined microscopically. The highest concentrations of the surfactants that did not produce any deleterious effect on these cells were tested. The effect of the surfactants on AAV vector capsids was also examined by including a 10% surfactant in the vector stocks (AAV-LacZ with serotype 2 capsid, 2 $\times$ 10^{10} VG/μl) for 24 hr; subsequently, the vector solutions were added to the cultured 293 cells in a 96-well plate at a dose of 2 $\times$ 10^4 VG/cell. The final concentration of the surfactants within the culture medium was 0.05%. Two days later, the infectivity was assessed by 5-bromo-4-chloro-3-indolyl-β-D-galactopyranoside (X-Gal) staining (Fan *et al.*, 1998).

Analysis of gene expression and of enhancing effect in vivo

For the *in vivo* experiments, the AAV vector solutions containing various concentrations of Pluronic F68, F88, and Tween 80 were injected into the subcutaneous adipose tissues of C57BLKS/J *db/db* mice (Japan SLC, Hamamatsu, Japan) at the age of 10 to 12 weeks. At the time of injection, the average weight of the animals was more than 50 g, and the subcutaneous adipose tissues were well developed. The AAV-CMV-LacZ vectors with various serotypes (serotype 1–5) were tested at a dose of 6 $\times$ 10^{10} VG/body. Two weeks after injection, the mice were killed, and their adipose tissues were enucleated, stained with 5-bromo-4-chloro-3-indolyl-β-D-galactopyranoside (X-Gal), cut into pieces, and then frozen with Tissue-Tek optimal cutting temperature (O.C.T.) compound (Sakura Finetek, Torrance, CA) in dry ice–ethanol, as described (Ogata *et al.*, 2004). When the tissue blocks were sliced for microscopic examination, they were also evaluated macroscopically and photographed. A densitometric analysis of the blocks was performed in order to substantiate the difference in the efficiency of transduction of adipose tissue under various injection conditions. In practice, five areas of the corresponding blocks were chosen and quantified, using Image Gauge software (version 3.0; Fuji Photo Film, Tokyo, Japan). After subtracting the background value, these numbers were analyzed and the statistical significance was evaluated. Experiments were performed with AAV-Epo vectors under conditions optimized with the AAV-LacZ vectors. Later, experiments at a higher vector dose (2 $\times$ 10^{11} VG/body) were included. On the basis of the preliminary experiments, the volume of injection was optimized as 100 μl/body (50 μl per lobe) and kept constant thereafter. Whole blood was collected from the tail vein every 2 weeks. Plasma Epo concentrations were quantified with an enzyme-linked immunosorbent assay (ELISA) kit (Roche Diagnostics, Mannheim, Germany). Complete blood counts were performed with a PC-608 particle counter (Erma, Tokyo, Japan).

Detection of murine Epo within adipose tissue of db/db *mice*

Adipose tissues were obtained from *db/db* mice at the time of sacrifice or later by operation. For the immunofluorescence study, adipose tissues were fixed and frozen in the presence of the O.C.T. compound in dry ice–ethanol, following which they were reacted with goat anti-human Epo (Santa Cruz Biotechnology, Santa Cruz, CA) and donkey anti-goat IgG conjugated with Alexa 488 (Invitrogen Molecular Probes, Eugene, OR) at 4°C for 16 hr to visualize murine Epo by fluorescence microscopy, as described in a previous report (Ogata *et al.*, 2004).

Detection of murine Epo transcript within adipose tissue by reverse transcription-polymerase chain reaction

Total RNA was isolated from adipose tissue with an RNeasy lipid tissue kit (Qiagen, Hilden, Germany) and was converted to

FIG. 1. Distribution of LacZ expression within adipose tissues. AAV-CMV-LacZ vectors of various serotypes (serotypes 1–5) were tested (n = 3 for each serotype) at a dose of 6 $\times$ 10^{10} VG/body. Two weeks after injection, adipose tissues were removed, stained with X-Gal, and resected in pieces. Tissues were frozen with Tissue-Tek and then cut into 20-μm-thick slices for microscopic analysis. Blocks were also evaluated macroscopically, photographed, and analyzed by densitometry. (**A**) Representative blocks of adipose tissue injected with various concentrations of Pluronic F88. (**B**) Densitometric analysis of the corresponding blocks with various concentrations of Pluronic F88. Asterisks indicate statistical significance ($p < 0.05$) compared with values of tissues without F88 (0% data). (**C**) Blocks of adipose tissue injected with serotypes of AAV-LacZ vectors with 2% F88. (**D**) Densitometric analysis of blocks corresponding to the serotypes of AAV-LacZ vectors. Double asterisks indicate statistical significance ($p < 0.05$) relative to values obtained with the rest of the serotypes. Microscopic analysis of adipose tissue sections transduced with AAV1-LacZ without excipients is shown at low (**E**) and high (**F**) magnifications. Adipose tissues transduced with AAV1-LacZ in the presence of 2% Pluronic F88 are shown at low (**G**) and high (**H**) magnifications.

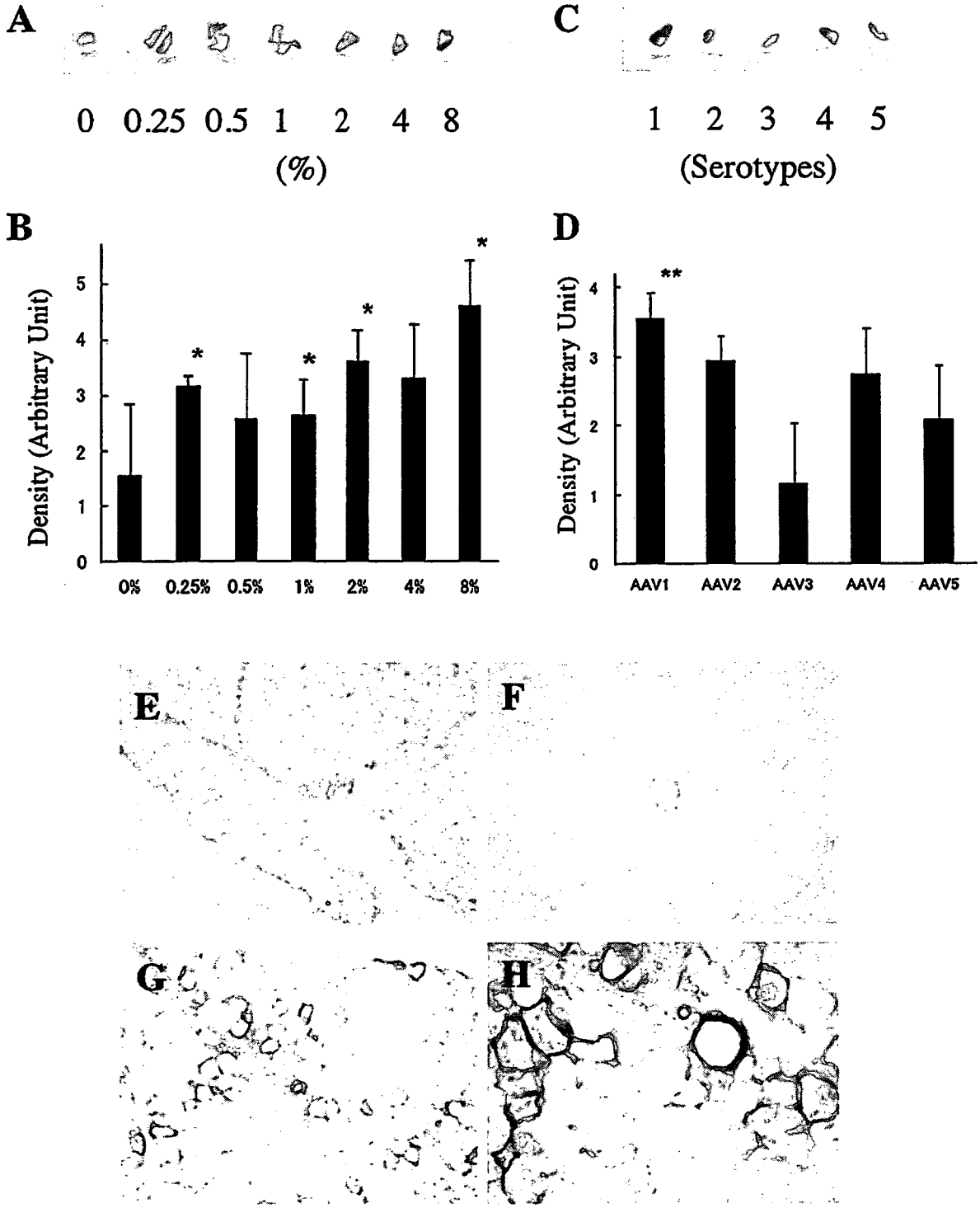
A
0 0.25 0.5 1 2 4 8
(%)
C
1 2 3 4 5
(Serotypes)
B
Density (Arbitrary Unit)
0 1 2 3 4 5
0% 0.25% 0.5% 1% 2% 4% 8%
D
Density (Arbitrary Unit)
0 1 2 3 4
AAV1 AAV2 AAV3 AAV4 AAV5
E
F
G
H

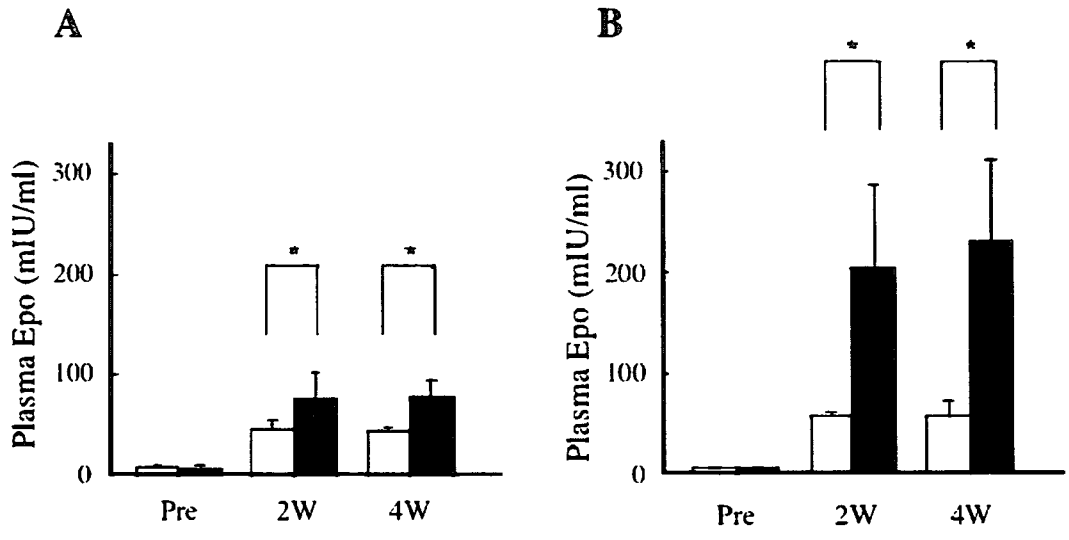

FIG. 2. Plasma Epo concentrations in *db/db* mice after injection of AAV1-Epo vectors into adipose tissue at a dose of (**A**) 6×10^{10} or (**B**) 2×10^{11} VG/body. Open and solid columns represent groups without and with 2% Pluronic F88, respectively, at the time of vector injection into adipose tissue. Each column and error bar indicate, respectively, the mean and SD of the group ($n = 5$). Asterisks indicate significance ($p < 0.05$).

cDNA with reverse transcriptase (SuperScript; Invitrogen, Carlsbad, CA) and oligo(dT) primers in a 20-μl mixture after DNase I (amplification grade; Invitrogen) treatment according to the manufacturer's instructions. Subsequent polymerase chain reaction (PCR) amplification was carried out with 1 μl of cDNA solution in a 50-μl reaction mixture containing 5 units of *Taq* polymerase, 10 m*M* Tris-HCl (pH 8.5), 50 m*M* KCl, 1.5 m*M* $MgCl_2$, and 100 μM dNTPs in the presence of specific primer pairs (200 n*M*) designed to amplify DNA fragments derived from the transcript of the mouse Epo transgene. Each PCR cycle involved denaturation at 94°C for 15 sec, annealing at 56°C for 30 sec, and extension at 72°C for 30 sec. The PCR products were analyzed by agarose gel electrophoresis. The authenticity of the PCR products was confirmed by observing their molecular sizes after agarose gel electrophoresis and by sequencing (ABI PRISM 310 genetic analyzer; Applied Biosystems, Foster City, CA). The primer sequences for mouse Epo were 5′-GTG CAG AAG GTC CCA GAC TGA GTG A-3′ and 5′-TTG GCG TAG ACC CGG AAG AGC TTG-3′. The primers for mouse glyceraldehyde-3-phosphate dehydrogenase (GAPDH) were purchased from Clontech Laboratories (Palo Alto, CA).

Removal of transduced tissue

AAV1-Epo vector solution (2×10^{11} VG/body) including 2% Pluronic F88 was injected into the subcutaneous adipose tissues of *db/db* mice. After 4 weeks, the adipose tissues were removed by standard surgical techniques under anesthesia. Plasma Epo concentrations were followed up 2 weeks thereafter. Four animals were analyzed and monitored.

Data and statistical analysis

Data are presented as means ± SD and were analyzed by Student *t* test after confirming an insignificant difference in variance between groups. $p < 0.05$ was considered statistically significant.

RESULTS

Screening of excipients in vitro

First, *in vitro* screening experiments were performed using nonionic surfactants. We tested Pluronic F68, F88, L72, P85, and Tween 80 for their effects on cell culture. Pluronic F68 and F88 were innocuous to cultured 293 cells at concentrations of up to 10 and 0.3%, respectively. The rest of the surfactants showed deleterious effects on the cultured cells when included at concentrations of 0.1% or higher. Next, we incubated AAV2-LacZ vectors with up to 10% Pluronic F68 and F88 solutions for 1 hr and checked their infectivity in 293 cells at 1×10^5 VG/cell. There were no differences in the infectivity of the vectors treated with these excipients, as assessed by X-Gal staining (data not shown).

Assessment of LacZ expression by use of Pluronics

On the basis of general safety data and *in vitro* experiments, we selected Pluronic F68, Pluronic F88, and Tween 80 as candidates for vector injection into *db/db* mice. Because preliminary experiments indicated the usefulness of Pluronic F88 combined with the AAV1 vector, we tested the usefulness of F88 at various concentrations. Comparison of blocks showed that there appeared to be an augmentation of LacZ expression with increasing concentration (Fig. 1A). The enhanced expression was substantiated by densitometric analysis of the blocks (Fig. 1B). On the basis of the result, we compared the usefulness of serotypes 1 through 5 combined with 2% Pluronic F88. The result showed that AAV1 was the most suitable serotype to trans-

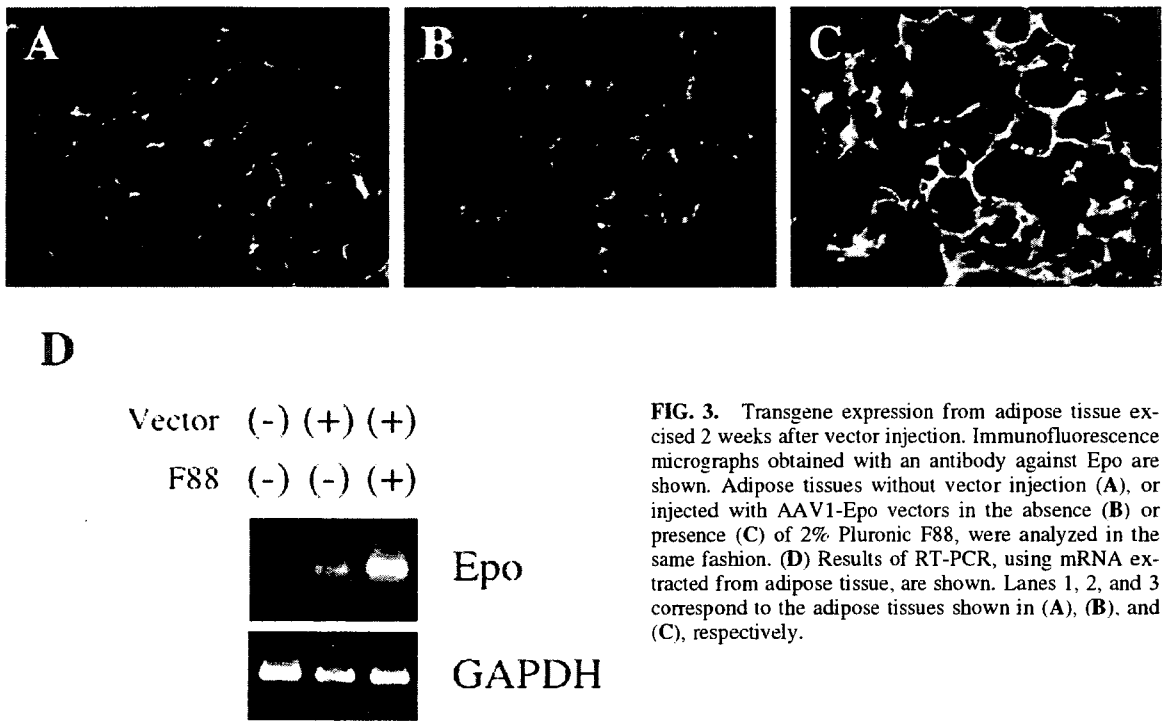

FIG. 3. Transgene expression from adipose tissue excised 2 weeks after vector injection. Immunofluorescence micrographs obtained with an antibody against Epo are shown. Adipose tissues without vector injection (**A**), or injected with AAV1-Epo vectors in the absence (**B**) or presence (**C**) of 2% Pluronic F88, were analyzed in the same fashion. (**D**) Results of RT-PCR, using mRNA extracted from adipose tissue, are shown. Lanes 1, 2, and 3 correspond to the adipose tissues shown in (**A**), (**B**), and (**C**), respectively.

duce adipose tissue *in vivo* (Fig. 1C and D). Enhancement of LacZ expression was also observed microscopically in the presence of Pluronic F88 (Fig. 1G and H) when compared with that of the vector alone (Fig. 1E and F).

Assessment of murine erythropoietin expression by use of Pluronic F88

On the basis of the findings obtained with LacZ vectors, we used vectors encoding murine erythropoietin (Epo) to demonstrate the enhancement of Epo concentration in a more quantitative manner. Increased plasma Epo concentration was observed 2 and 4 weeks after vector injection, and there was enhancement of Epo in the presence of 2% Pluronic F88 at a dose of 6×10^{10} VG/body (Fig. 2A). At a higher dose of 2×10^{11} VG/body, the enhancement effect was more prominent (230 ± 80 versus 58 ± 14 mU/ml at 4 weeks; Fig. 2B).

Assessment of transgene expression within adipose tissue

In the histological analysis of transduced tissues, a significant enhancement of Epo expression was observed by immunofluorescence when 2% F88 was included in the vector solution (Fig. 3A–C). Results of reverse transcription (RT)-PCR also showed enhanced expression of murine Epo in the presence of 2% F88 (Fig. 3D). Tissue damage or cellular infiltrates were not observed in the transduced adipose tissues throughout the histological evaluation (data not shown).

Effect of removal of transduced tissue

Bilateral lobes of abdominal adipose tissue were selected as a target for transduction. Plasma Epo concentrations were monitored after injection of AAV1-Epo vector (2×10^{11} VG/body) with 2% F88. After 4 weeks of observation, both lobes of the adipose tissue were removed *en bloc*, using standard surgical techniques. A significant decrease in plasma Epo concentration was observed 2 weeks after operation, with a return to the baseline level (Fig. 4). In addition, mice after removal of transduced tissue showed extended survival compared with "non-operated" mice. The survival period of *db/db* mice is summarized in Table 1.

DISCUSSION

In this study, we demonstrated the advantages of using excipients in adipose tissue transduction with AAV vectors. In practice, Pluronics have been widely used as excipients, including for administration to humans (APhA and RPSGB, 1986). Generally, one of the most frequent complications associated with administering a surfactant *in vivo* is hemolysis. With regard to this, it is noteworthy that Pluronics have a membrane-protecting effect on erythrocytes and that Pluronic F68 has long been used as a drug to prevent hemolysis and thrombotic events during extracorporeal circulation (Wright *et al.*, 1963). Further, their efficacy for use in the treatment of vasoocclusive disease in sickle cell anemia is currently being evaluated (Gibbs and Hagemann, 2004). Pluronics are also used in

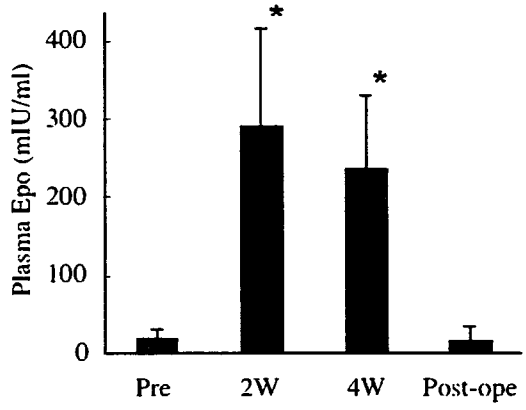

FIG. 4. Plasma Epo concentrations of *db/db* mice after injection and removal of adipose tissue. AAV1-Epo vectors were injected into adipose tissue at 2×10^{11} VG/body with 2% Pluronic F88. Four weeks after injection, transduced adipose tissues were surgically removed and monitored for an additional 2 weeks. Columns and bars indicate, respectively, mean ± SD of the groups ($n = 4$ each). Asterisks indicate significance ($p < 0.05$) relative to concentrations before injection. No significant differences in concentrations were observed 2 weeks after the operation relative to concentrations before injection.

a variety of applications in gene therapy; for example, they are used to augment gene transfer into cultured cells (Gebhart and Kabanov, 2001), to protect skeletal muscle membranes at the time of electroporation *in vivo* (Lee *et al.*, 1992; Hartikka *et al.*, 2001), and to enhance adenovirus-mediated gene transfer into the lungs (Croyle *et al.*, 2001). In addition, it has been postulated that adding a low concentration (0.01%) of Pluronic F68 into the stocks of AAV vectors prevents vector loss by reducing nonspecific attachment (Sommer *et al.*, 2003).

In the present study, the efficiency of gene transfer into adipose tissue was augmented by the use of Pluronic F88. The mechanisms behind this phenomenon are not clear; however, it is known that Pluronics improve the distribution of a solution and its content (APhA and RPSGB, 1986). In a previous study, one member of the Pluronics family (poloxamer 407) was shown to improve the efficiency of adenovirus-mediated gene transfer to arterial smooth muscle cells (Feldman *et al.*, 1997). A reduction in incubation time from 20 to 10 min to attain the same level of gene transfer by including this excipient was also demonstrated. The following two possible mechanisms were postulated for the increase in efficiency of gene transfer: (1) the formation of a transient local reservoir for the sustained release of adenoviral vectors, or (2) acceleration of the uptake of adenoviral vectors produced by the interaction between poloxamer 407 and the cell membrane. On the basis of our observations concerning LacZ expression within adipose tissues (Fig. 1), it can be said that vector distribution was improved and that uptake of the vectors was facilitated. The augmentation was most significant in the case of AAV1 vectors, as assessed on the basis of both LacZ and Epo. There may be a specific advantage in combining the AAV1 capsid with Pluronic F88 when transducing adipose tissue.

A novel action of Pluronics has been reported (Sriadibhatla *et al.*, 2006). In this literature, transcriptional activation of transgenes driven by the CMV promoter or nuclear factor-κB (NF-κB)-responsive elements was demonstrated in the presence of Pluronics. As all the vectors in our current study used the CMV promoter, transcriptional activation through this mechanism might be a concern. Therefore, this issue needs to be taken into consideration. In the literature, all the transcriptional activation was observed in *in vitro* experiments, and Pluronics were continuously present within the culture medium, typically at levels of 0.1% or higher. On the other hand, in our experiments, Pluronics were administered only at the time of vector injection, and the net amount constitutes 0.004% of the total body weight based on the volume and concentration of the vector solution. Moreover, the half-life of Pluronics *in vivo* is estimated as some hours and the majority of the administered material is known to be excreted from the urine within days (APhA and RPSGB, 1986; Gibbs and Hagemann, 2004). Therefore, it is unlikely that transcriptional activation is responsible for gene expression *in vivo* weeks after administration. Nonetheless, this mechanism of action may potentially be useful in order to enhance the outcome of gene therapy approaches *in vivo*. As all the known regulatable gene expression systems share the weakness of toxicity (Goverdhana *et al.*, 2005), safety profiles of Pluronics along with rapid clearance from the body may lead to the development of a novel system for regulatable gene expression *in vivo*. Further studies in this respect may extend the utility of Pluronics in future.

A relatively small number of studies have reported successful gene transfer into adipocytes. There are reports on gene transfer into cultured adipocytes by using viral vectors such as adenovirus (Meunier-Durmort *et al.*, 1996, 1997; Hertzel *et al.*, 2000), lentivirus (Morizono *et al.*, 2003; Carlotti *et al.*, 2004), and retrovirus (Ito *et al.*, 2005). Regarding efficacy *in vivo*, gene transfer into gonadal adipose tissues, using adenoviral vectors, demonstrated clinical efficacy in treating diabetic conditions (Nagamatsu *et al.*, 2001). Successful transduction of adipose tissue by using either simian immunodeficiency viral vector (Ogata *et al.*, 2004) or herpes simplex viral vector (Fradette *et al.*, 2005) was reported. To our knowledge, this is the first report that demonstrates the efficacy of adipocyte-mediated gene transfer by AAV vectors.

In terms of vector dose, adipocyte-mediated gene transfer required a higher vector dose to achieve the same plasma Epo

TABLE 1. LENGTH OF SURVIVAL OF *db/db* MICE

Group	*Survival (weeks after injection)*
AAV1-Epo (no Pluronic F88)[a]	4,[b] 4, 6, >8,[c] >8[c]
AAV1-Epo + 2% Pluronic F88[d]	4, 4, 5, 6, >8[c]
AAV1-Epo + 2% Pluronic F88 + operation[e]	>24, >24, >24, >24

[a]Reflects animals in Fig. 2B (open columns).
[b]This animal became paralyzed at the time of blood collection and subsequently died.
[c]These animals were killed at week 8 for tissue analysis.
[d]Reflects animals in Fig. 2B (solid columns).
[e]Reflects animals in Fig. 4.